Chapter 5

Determination of Copper (II) ions in multivitamin tablets after enhancement of mass transfer across the neutral membrane and the preconcentration of the dialysate ions.

5.1 Introduction

In chapter 4, the right of existence of the use of an electrodialyser (ED), equipped with a neutral, passive membrane, was established for use in an anion, flow injection analysis (FIA) system. The aim of the investigation was expanded to include the use of the above mentioned ED system for use in a cation FIA system. The main objective of this part of the study was to evaluate the use of the ED system incorporated into an FIA system for the analysis of a cation. A prerequisite for the detector used was its compatibility with the ED/FIA system, the detection limit and also the rate at which the sample could be analysed.

Various methods of determination of copper ions in FIA systems have been exploited. Most commonly used method was the direct determination of the copper ions by means of spectroscopic methods. Atomic spectrometry is one of the most sophisticated and elegant methods for direct assay of cations. [1] Flame atomic absorption spectrophotometry (FAAS) is used extensively in FIA systems. [2-14] The graphite furnace [15 -17] and the Inductively Coupled Plasma (ICP) [18 - 21] as a means of detection was also often used. Other methods used includes electrochemical methods [22 - 25], and also the reactions of copper ions with a colour reagent and detection of the coloured product with a UV/Vis spectrophotometer [36 - 30].

The obvious choice was the use of the FAAS detector. It gave a direct and fast determination of the copper ions with very few interferences. [1] Direct determination (without sample pretreatment) could give a sampling rate of as high as 150 samples per hour. [1] The use of a colour reagent gave a lower sampling rate (due to the reaction

that had to take place) but higher detection limits than the FAAS. [31] The use of electrochemical detectors were not advised due to the interference of the ED system on the detector (as was also experienced in chapter 4).

The use of flow injection (FI) techniques for the preparation of solutions prior to their aspiration into atomic spectrometry systems forms the basis of interfaced flow injection-atomic spectrometry. Although FI has become a well-known name to most chemists over the past two decades, the real success of practical instrumental FI analysers in routine analytical laboratories and process analysers depended on the type of basic components used, and the construction thereof into a working FI system. It is apparent, from the above mentioned FAAS literature, that a very wide variety of different on-line manipulations of samples and standards had been carried out by FI techniques and that the combination with conventional FAAS enhanced the performance of an analytical method. The most prominent example of such on-line sample pretreatment was the preconcentration of the analyte on an ion-exchange column built into the conduits of the FIA system as was illustrated by Hirata *et al* [3], Purohit and Devi [4], Naghmush *et al* [7], Burguera *et al* and Van Staden and Hattingh [13]. Other very effective ways of preconcentration (not necessarily used in FIA/FAAS systems) were the use of immobilised micro organisms (which was done by Elmahadi and Greenway [9] and Maquieira *et al* [10, 11, 32]), solvent extraction as illustrated by Kuban *et al* [2] and precipitation by Zhuang *et al* [16] and Esmadi *et al* [33].

Active or Donnan dialysis is a promising technique for the preconcentration, recovery and speciation of ionic species, but with a limitation in the amount of mass transfer of species through the membrane. Cox and co-workers [34 - 36] worked for many years on sample preparation on an analytical scale using Donnan dialysis, employing the technique for matrix normalization [34] and sample preconcentration. [35, 36] Active dialysis was also used as a preconcentrating technique by Koropchak and co-workers. [37, 38]

In the case of passive dialysis, very little work was done to circumvent the

disadvantages of the dilution of the analyte during its passage over the neutral membrane. It is evident, from the experimental work mentioned in chapter 4, that there was a substantial increase in the percentage dialysis with the incorporation of the electrodialyser. Still there is a massive dilution factor since, at its best, the percentage dialysis was found to be only 37 %. The preconcentration methods, described earlier in this chapter, can of course be used with great success by preconcentrating the dialysate ions before detection in the FI system. Kuban et al. [39] used solvent extraction to preconcentrate copper in an FI manifold before detection with FAAS, although normally ion-exchange resins are used for on-line preconcentration in FI systems. Carbonell et al. [40] compared various cation-exchange resins which are commercially available. Using liquid chromatography (LC), Turnell and Cooper [41, 42] first dialysed the sample after which it was derivatized or preconcentrated before injection into the LC system. Preconcentration, using an ion-exchange column after dialysis in an FI system was also employed by Van Staden and Hattingh. [13] The detection limit was decreased dramatically, although most of the analyte ions in solution were lost due to the low efficiency in mass transfer over the neutral membrane. There was no improvement in the percentage dialysis.

The properties of electrodialysis make it potentially applicable to quantification of trace ions in samples which require a prior separation and/or enrichment step and this was evaluated by Cox and Carlson [43] as an active preconcentration method. These workers demonstrated that electrodialysis can be employed for ion enrichment and also that, compared with Donnan dialysis, higher enrichment factors are attained. However, for enrichment of trace ions in samples, the quantification procedure is not straightforward and for very low analyte concentrations internal standard an/or ionic strength normalization methods were required in order to obtain reasonable precision. Van Staden and Hattingh [48] not only encountered the same problem when employing active dialysis membranes as part of their electrodialyser-FI system, but also found that the ion-exchange properties of the Donnan ion-exchange membrane became predominant and the main hindrance to obtaining a reasonable accuracy and precision.

5.2 Experimental

5.2.1 Reagents and solutions

All reagents were prepared from analytical-reagent grade chemicals unless specified otherwise. De-ionised water from a Modulab system (Continental Water Systems, San Antonio, TX, USA) was used for dilution. All solutions were de-gassed with a vacuum pump system before measurement. The solutions were prepared as follows:

A stock standard solution containing 10 000 mg ℓ^{-1} copper(II) ion was prepared by dissolving 78.585 g of copper sulfate pentahydrate in de-ionised water and diluting to 2000 mℓ with de-ionised water.

A 1.0 mol ℓ^{-1} HNO_3 solution was prepared by diluting 42.3 mℓ of a 11.7 mol ℓ^{-1} HNO_3 solution (sp. gr. 1.34) to 500.0 mℓ.

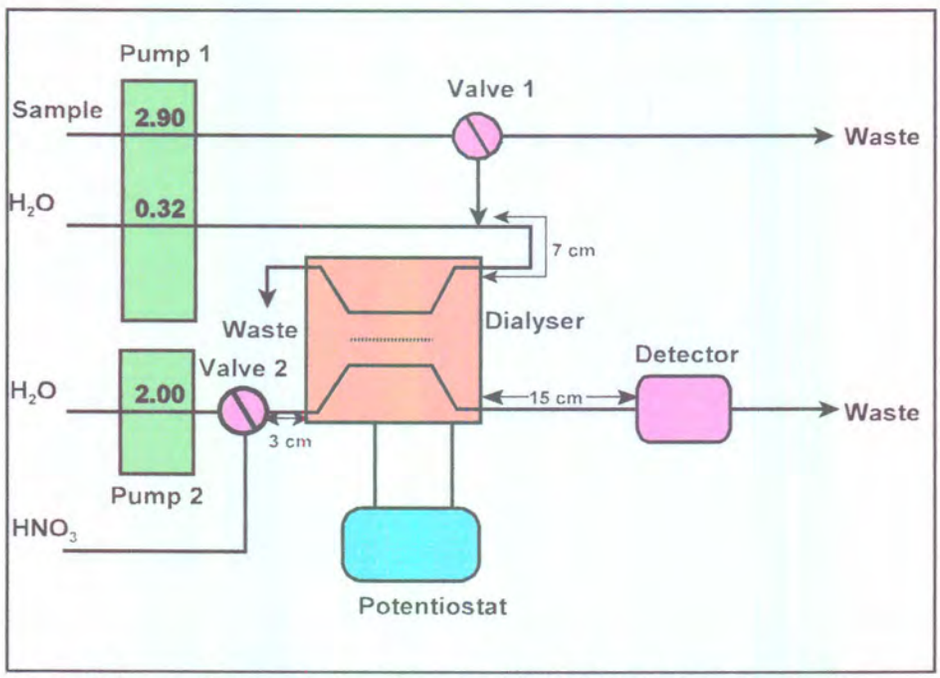

Figure 5.1 Schematic flow diagram of the ED-FI-AAS system for the determination of copper.

5.2.2 Instrumentation

The FI system (Figure 5.1) used was composed of the following components:

1. Two six-roller Cenco peristaltic pumps (rotating at 10 rev min^{-1}). The first pump, P1, was used to draw up sample and flow in the donor stream. This pump was never switched off during the analysis. The second pump, P2, was used for the flow of the deionised water in the acceptor stream. The HNO_3 stream was not transported by a pump, but was drawn up by the Atomic Absorption Spectrometer (AAS) burner.
2. Two Valco (Houston, TX, USA) 10-port electrically actuated injection valves. The first Valco valve, with a sample loop of 80 µℓ, was used to inject the sample into the donor stream whereas the

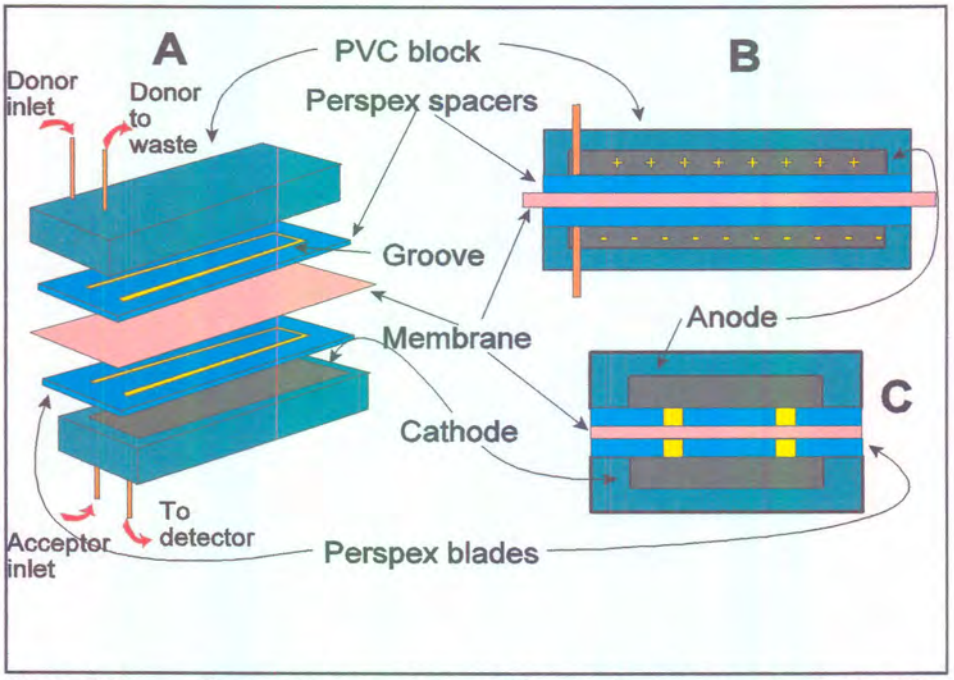

Figure 5.2 *Schematic presentation of the Electrodialyser unit. A - the 3D presentation, B - a longitudinal cross-section and C - a diagonal cross-section.*

second Valco valve was used to select between the H_2O stream from pump 2 and the HNO_3 stream, which was used to flush the acceptor stream.

3. The manifold consisted of Tygon tubing, with an id of 0.76 mm, cut into the required lengths and wound around glass tubes with an od of 10 mm.

4. The electrodialyser unit used (Figure 5.2) was a slightly modified version of the dialyser previously described by van Staden and van Rensburg [45] and modified into an electrodialyser unit. It is similar to the one used in chapter 4 for the determination of chloride with the only difference that the polarity on the electrodes were swopped so that the anode was situated in the donor channel and the cathode in the acceptor channel. The dialyser unit consisted of two, mirror image, PVC blocks. Embedded into each of these blocks were graphite electrodes which acted as the anode (acceptor side) and the cathode (donor side) respectively. Placed onto each of the PVC blocks was a 0.6 mm thick Perspex blade. Into each of the Perspex blades, a groove of 0.6 mm width and 300 mm length was cut so as to form a channel when placed onto each of the PVC blocks respectively. The PVC blocks were then fitted onto each other in such a way that the Perspex blades facing each other and the grooves in the respective Perspex blades coincided with each other. The membrane was then sandwiched between the two Perspex blades as the only separation between the two channels so formed. The walls of the channels that were formed thus consisted of, at the far end, the graphite (which was embedded into the PVC blocks), the side walls of Perspex and the common wall, the membrane. A Spectrapore passive (MW cut-off 6000-8000, pore size 2.5 - 4 nm, thickness 0.031 mm) was used

in the dialyser unit.

5. A Leader LPS 156 potentiostat was used to apply the dc potential.

6. For current and potential measurements a Prema 5000 integrating multimeter was used.

7. The detector used was a Varian (Palo Alto, CA, USA) AA-1275 atomic absorption spectrometer. A Varian Techtron Cu hollow cathode lamp, with a current of 10 mA, was used to give a monochromatic light ray in the detector. A wavelength of 324.7 nm and a spectral bandpass of 0.2 mm was used. A lean (oxidising) air-acetylene flame was used.

8. The AAS detector, the pumps and the valves were coupled to a personal computer equipped with the FlowTEK program. [48]

5.2.3 Flow system

The flow system used is depicted in Figure 5.1. The sample solution was drawn up into an 80 µℓ sample loop of the Valco valve 1 from where it was injected into the carrier donor stream and transported to the electrodialyser. Analytes in the sample donor stream were electrodialysed under the influence of an applied potential through the passive neutral membrane to the acceptor channel, which was stagnant at this time. The dialysed copper ions in the acceptor stream were further plated onto the cathode under the influence of the dc potential. After a certain fixed period of electrodialysis, the acceptor channel was flushed with the HNO_3 stream, dissolving the plated copper metal zone on the cathode, and transporting it directly to the AAS detector. The direction of flushing of the acceptor channel was countercurrent to the flow in the donor channel. Data acquisition and device control were achieved using a PC30-B interface board (Eagle Electric, Cape Town, South Africa) and an assembled distribution board

(MINTEK, Randburg, South Africa). The FlowTEK [48] software package for computer-aided flow analysis was used throughout for device control and data acquisition. All the data given (mean peak area values) are the average of 11 repetitions.

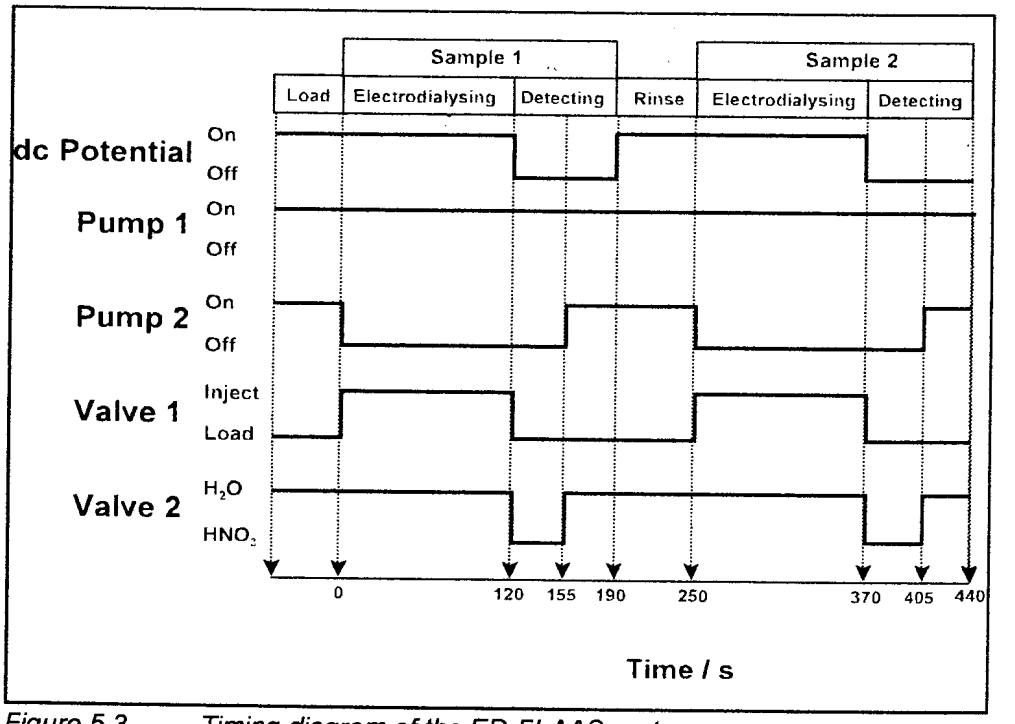

Figure 5.3 Timing diagram of the ED-FI-AAS system

5.2.4 Procedure

The configuration of the FI system is shown in Figure 5.1. The pump and valves operated as described below.

5.2.4.1 Operation of pump and valves

Pumps where either in operation or switched off. Pump P1 (Figure 5.1) was never switched to the "off" position during the analysis. Pump P2 (Figure 5.1) was switched between the "on" and "off" positions at certain intervals. Two types

was used to channel either the HNO_3 solution or de-ionised water through the acceptor stream of the dialyser. A Valco 10-port electrically actuated injection valve (V1 in Figure 5.1) was arranged in such a way that it served as a sampling valve with a sample loop of 81 µℓ. In the "load" position, sample was aspirated through the sample loop to waste filling the whole sample loop. Upon switching to the "inject" position (which was time-regulated with pump P2), part of the donor stream was interrupted and the full sample loop was placed into the donor stream. A Valco 10-port electrically actuated valve (V2 in Figure 5.1) was arranged in such a way that it could be switched between the H_2O and HNO_3 channels feeding the acceptor channel of the electrodialyser at certain intervals (see Figure 5.3).

The timing diagram for treating the samples is outlined in Figure 5.3. The system was switched on and allowed to run for about 10 min in order to equilibrate the flow dynamics of all parts of the system. The computer was then actuated and the timing sequence started in the "load" position which was only used at the beginning of the analysis. The following timing sequences were followed with time regulation from the FlowTEK [48] program:

i. *Starting of the system (Loading)*

Pumps: Pumps P1 and P2 were switched to the "on" position. Pump P1 pumped H_2O through the donor channel at a rate of 0.32 mℓ min^{-1} and the aspirated sample (sample 1) into the sample loop at 2.90 mℓ min^{-1}.

Valves: Valve V1 was in the "load" position and valve V2 directed H_2O at a flow rate of 2.00 mℓ min^{-1} through the acceptor channel of the ED.

Potentiostat: Potentiostat was set to "on" position at 15 V (see Figure 5.1)

ii. *Electrodialysis*

At time T = 0, pump P1 was kept in the "on" position and pump P2 was switched to the "off" position. For the whole duration of the electrodialysis period the flow in the acceptor channel was stopped. Valve V1 was switched to the "inject" position and the whole sample in the loop was inserted into the donor stream. This whole sample plug was then pumped through the donor stream of the dialyser at a flow rate of 0.32 mℓ min^{-1} where electrodialysis occurred. The applied potential over the membrane was kept at 15 V for the duration of the electrodialysing step.

iii. *Detection*

At time T = 120 s, the applied potential was switched off and valve V2 switched to the HNO_3 stream, allowing the detector to draw the HNO_3 with the electrodialysed dissolved copper(II) ion zone through the acceptor channel. The computer also started to read the signal coming from the detector. At time T = 155 s, valve V2 was again switched to H_2O and pump P2 actuated to pump the remaining dissolved analyte to the detector at a flow rate of 2.00 mℓ min^{-1}.

iv *Completion of a run*

At time T = 190 s, the computer stopped measuring the signal from the detector. The potentiostat was again switched on at 15 V. The donor and acceptor channels were rinsed and the next sample was aspirated into the sample loop. At T = 250 s, sample 2 was injected and the analysis of sample 2 started.

5.3 Results and discussion

Van Staden and Hattingh [46] previously tried to use anion-exchange membranes with the electrodialyser-FI system for the determination of chloride, but experienced the same problems as Cox and Carlson. [47] The ion-exchange properties of the Donnan ion-exchange membrane became predominant and a main hindrance to obtaining a reasonable accuracy and precision. They again tried cation-exchange membranes with the electrodialyser-FI-AAS system for the determination of copper(II) ions, but unfortunately, were not very successful, for the same reasons mentioned above. It was then decided to keep to the passive neutral membranes used previously (as was described in Chapter 4) and to try to improve on the performance.

In order to enhance the mass transfer of the copper cations over the passive neutral membrane as an accurate and precise measurable product, optimum system conditions were of the utmost importance in the design and operation of the electrodialyser-FI-AAS system. The first aim of this investigation was to draw the maximum amount of copper ions across the neutral membrane into the conduits of the acceptor channel by applying a dc potential gradient across the two sides of the membrane at optimum flow rates. The second goal was to allow the copper ions to accumulate in the acceptor channel where the copper was preconcentrated into a smaller zone before it was transported to the detector. To evaluate and optimise the preconcentration of the copper, a knowledge of the form in which the copper was concentrated in the acceptor stream was needed. Experimental work confirmed that copper metal was plated onto the cathode. (Confirmation was done by rinsing the acceptor channel of the dialyser unit extensively with de-ionised water. The water was then tested for traces of copper ions. Hereafter the acceptor channel of the dialyser unit was rinsed with a solution of nitric acid. It was found that the nitric acid solution contained copper ions after the rinsing of the acceptor channel)

Hereafter, the remainder of the system was optimised in as far as the following points were concerned: (i) flow rate of the donor channel, (ii) applied potential over the membrane, (iii) injection loop volume, (iv) flow direction of the donor and acceptor channels and (v) interferences.

5.3.1 Flow rate of the donor stream

The flow rate of the donor stream was an important parameter which had an influence on the electrodialysis efficiency. High flow rates prevented the transfer of the bulk of copper ions through the membrane to the cathode, while low flow rates resulted in a decrease in sample frequency. The applied dc potential was kept constant at 10 V during the optimisation of the donor flow rate. The acceptor channel flow was also stopped during the time set aside for the electrodialysis process to take place (Figure 5.3). The flow rate of the donor channel was varied between 0.10 and 0.60 mℓ min^{-1}. The influence of the flow rate of the donor stream was evaluated on the basis of the %RSD and peak area as illustrated in Figure 5.4. From Figure 5.4A it follows that the lowest %RSD was obtained at a flow rate of 0.32 mℓ min^{-1}. It is also apparent from Figure 5.4B that the lower the flow rate, the higher the peak area. It is evident from Figure 5.4B that there was a drastic decrease in peak area when the flow rate increased above 0.35 mℓ min^{-1}. The best compromise between the sensitivity and reproducibility was found at a flow rate of 0.32 mℓ min^{-1}.

5.3.2 Applied potential

The applied potential was evaluated using the detector signal for response (or the percentage electrodialysis) and the %RSD as indicators. The applied dc potential was a very important factor that determined the oxidation state into which the copper was preconcentrated in the acceptor stream. The applied dc potential was varied between 0 and 20 V, while the flow rate of the donor stream was kept constant at 0.32 mℓ min^{-1}. Figure 5.5 clearly indicates the state of the copper in the acceptor stream at different applied dc potentials. Figure 5.5 was obtained from the detector reading in the detection step in Figure 5.3. The moment the acceptor stream is allowed to be rinsed, all the Cu^{2+} ions would be transported towards the detector. (Since during the preconcentration step, only de-ionised water is present in the acceptor channel.) The copper that was plated on the cathode however, will lag behind since it had to be dissolved by the HNO_3 that was used to rinse the acceptor channel. For this reason at lower applied dc potentials not all of the copper ions were plated onto the cathode. The redox

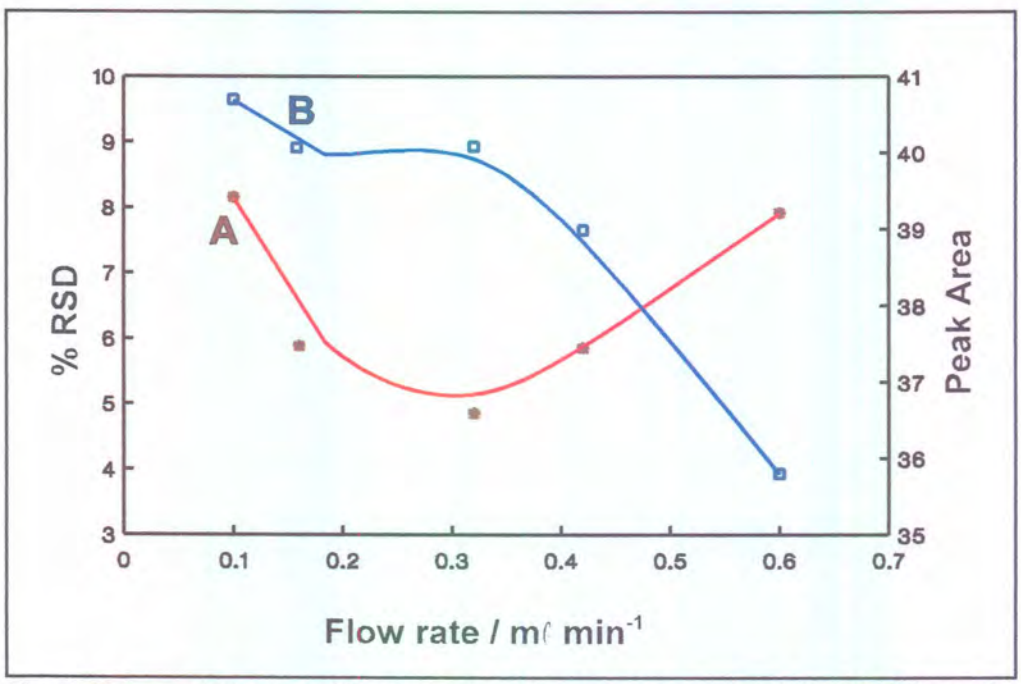

Figure 5.4 *Influence of the flow rate of the donor stream on* A *the %RSD and* B *the peak area.*

reaction for the plating of the copper is the following:

$$Cu^{2+}\ (aq) + 2\ e^- \rightarrow Cu\ (s) \quad E^\circ = 0.337\ V \text{ (at standard conditions)}$$

It is obvious that the applied potential (in Figure 5.5) would have been more than ample for the copper ions to be plated onto the cathode. It is evident from Figure 5.5 that at 5 and 10 V, the copper was in the Cu^0 and in the Cu^{2+} states. At these potentials not all the ions were plated since the migration rate at these potentials was too low for the ions to came into contact with the cathode. At a potential of 15 V however, all the copper ions were converted to the Cu^0 state. For this reason it was advisable always to work at applied potentials of 15 V and higher. The results in Figure 5.6A revealed that the precision increased with an increasing dc potential from 0 to 20 V. The reason for the sharp decrease in the %RSD at a dc potential higher than 10 V is because the bulk of the copper(II) is reduced to Cu(s) at higher dc potentials, whereas some copper is still in the Cu^{2+} oxidation state at lower dc potentials. When looking at the % electrodialysis

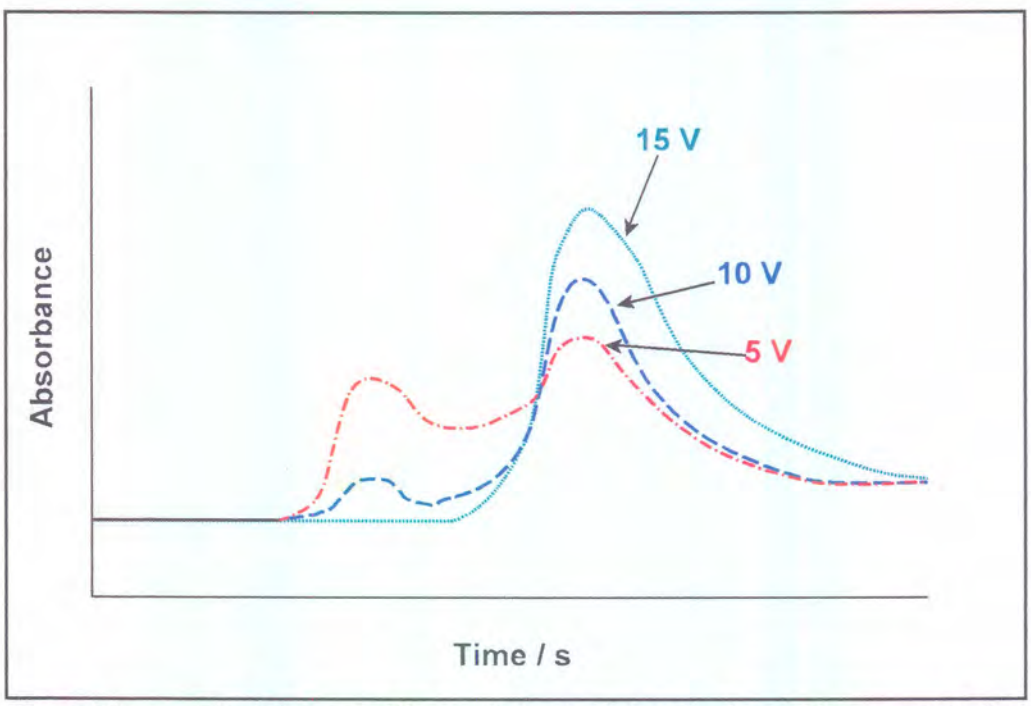

Figure 5.5 *The influence of the applied potential on the form of the copper in the acceptor channel.*

versus the applied dc potential (Figure 5.6B), it is apparent that the optimum dc potential is at 10 V. A further increase in the applied dc potential did not increase the percentage electrodialysis significantly. To compensate, however, for the better precision obtained at the higher applied dc potential and to ensure that all the copper was in the Cu^0 state, a value of 15 V was selected as the optimum.

The optimisation of the applied potential can also be influenced by the membrane potential and the flux of the analyte ions through the membrane. The membrane potential is an indication of the degree of fouling of the membrane as previously described Schoeman and co-workers [51 - 53]. This property was not investigated any further since problems with fouling were not encountered. The flux of the ions over the membrane is, however, also closely related to the applied potential and can therefore also be used as an indicator for choosing the optimum applied dc potential. The results obtained in Figure 5.7 (applied potential *versus* change in current) showed a sharp change in current when the applied potential was increased from 5 to 15 V, which indicated an increase in the flux of analyte ions through the membrane. There was a tendency for the change in current to drop above an applied potential of 15 V, which confirmed that a definite optimum was reached at 15 V.

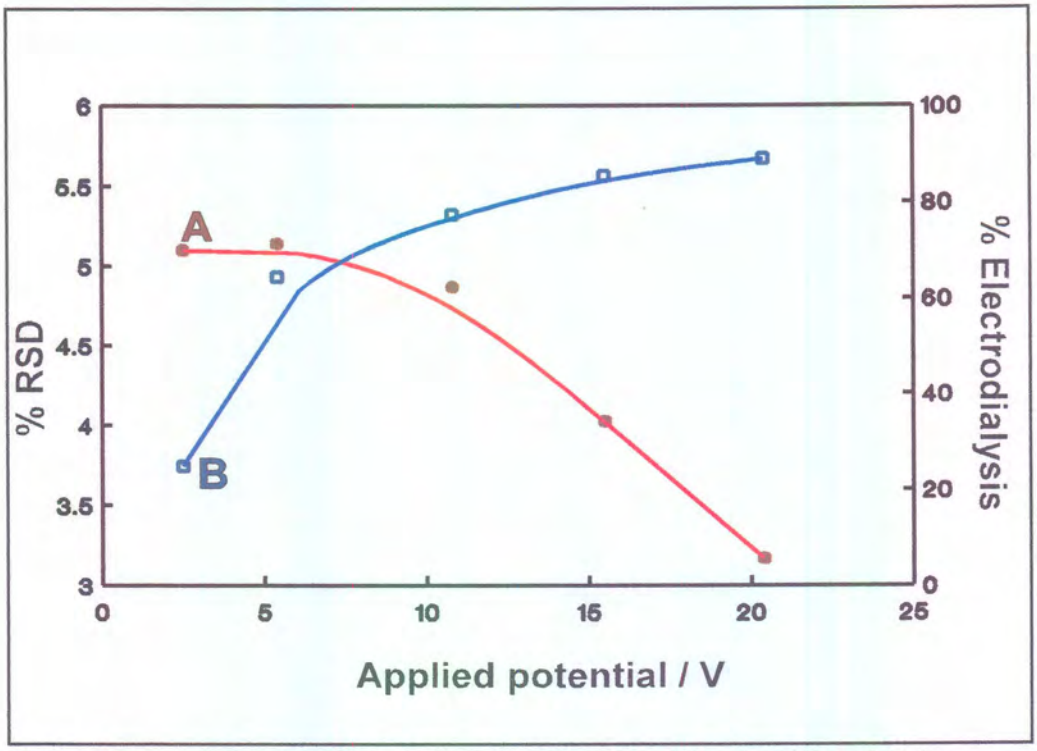

Figure 5.6 *Influence of the applied dc potential on A the % RSD and B the percentage electrodialysis.*

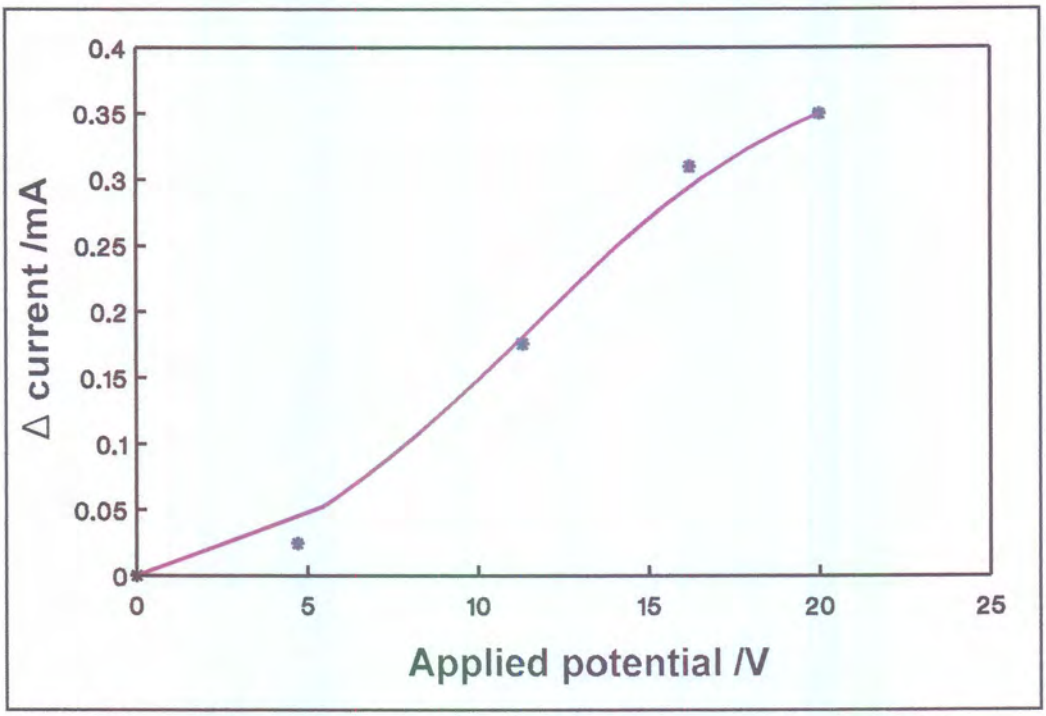

Figure 5.7 *Effect of the applied dc potential on the change of current in the acceptor channel indicating the flux of ions through the passive neutral membrane.*

5.3.3 Injection loop volume

The purpose in the evaluation of the volume of the injection loop was to find a sensitive method in the minimum time period involved for each run. It is evident from Figure 5.8 that the sensitivity of the system increased steadily with an increase in the volume of the injection loop. Thus by increasing the injection loop volume, the detection limit could be altered to fit a specific application. Unfortunately, the time involved for each run also increased with the increase in the volume of the injection loop. Thus, depending on the application, a compromise had to be found between the timing of each run and the sensitivity of the method. A sample loop volume of 80 µℓ gave ample sensitivity for the proposed system for the specific application and samples to be analysed and was, therefore, chosen for further work.

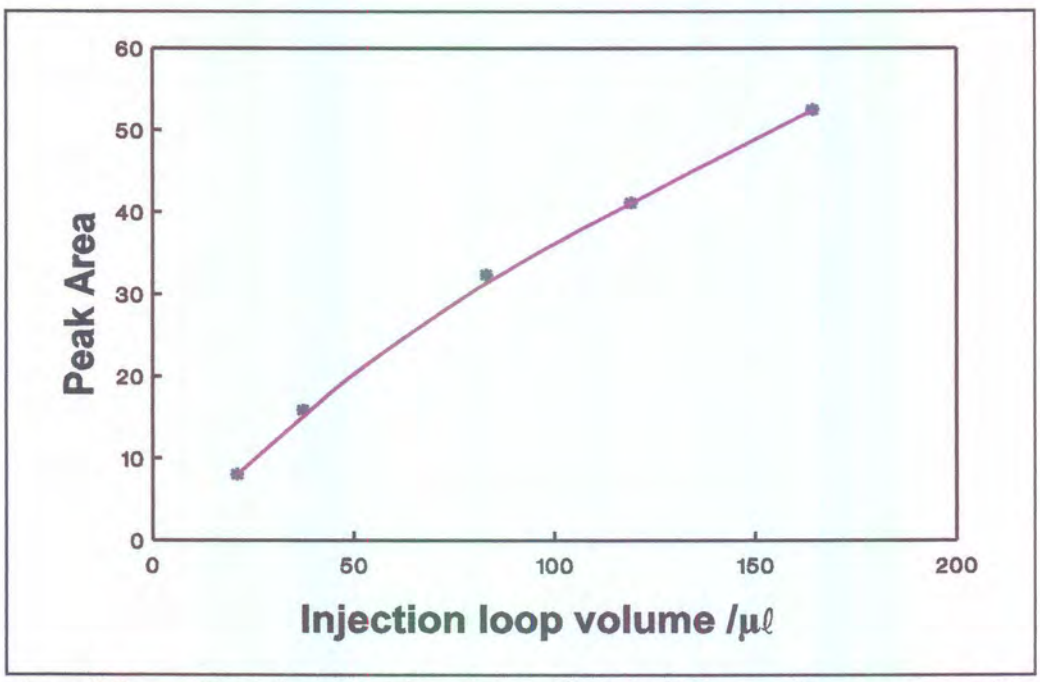

Figure 5.8 *The influence of the volume of the injector loop on the response of the system.*

5.3.4 Flow direction of the donor and acceptor channels

Under conventional FI-dialysis conditions, it was found that co-current movement of the donor and acceptor streams gave the best results. [17, 47 - 49] In this case it was found, however, that countercurrent movement of the donor and acceptor streams gave the best results, especially concerning RSD values. The moment the copper ions in the sample plug entered the electrodialyser in the donor channel, the majority of copper was immediately drawn as a narrow zone onto the cathode on the acceptor channel side as illustrate in Figure 5.9. Most of the plating occurred in the acceptor channel immediately opposite the entrance of the donor stream. After the electrodialysis mode, the acceptor channel was rinsed with nitric acid in the detection mode. (See Figure 5.3) If the acceptor channel was rinsed with the flow of the donor and acceptor streams counter currently, the dissolved copper ions would immediately be flushed out of the entrance of the acceptor channel as a plug with much less dispersion than would be the case with co-current rinsing as illustrate in Figure 5.9.

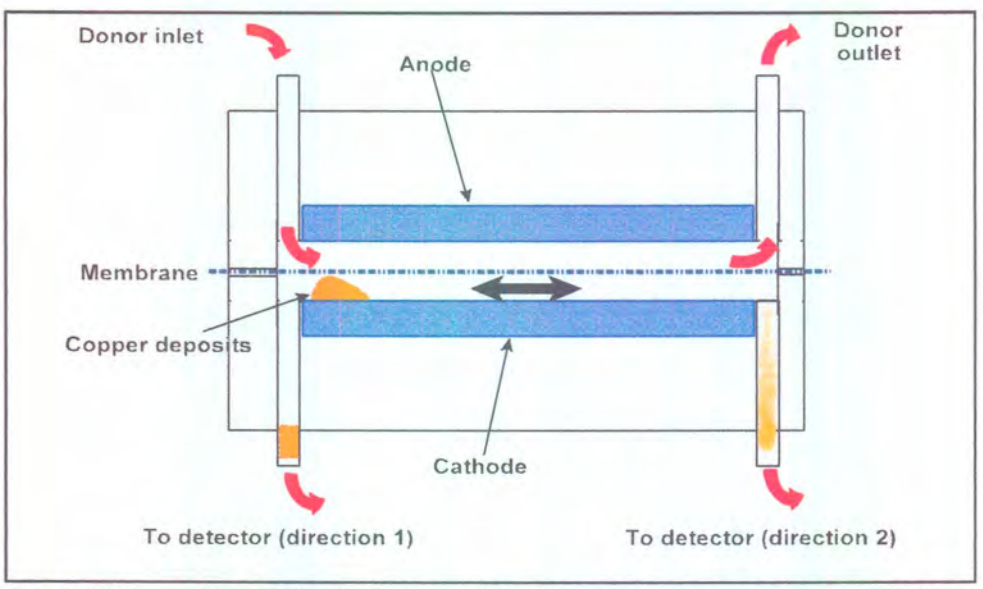

Figure 5.9 *Schematic illustration of the dispersion of the copper zone in the acceptor channel with countercurrent (direction 1) and co-current (direction 2) flow directions of the donor and the acceptor channels.*

5.3.5 Interferences

Interference could be divided into those interferences involving the electrodialysis system, the electrochemical system and those concerning the AAS detector. The main experimental work was concentrated on the interferences that may arise from the electrodialysis system. The interferences that could arise from the electrochemical system are those species that has a standard reduction potential of higher than 0.337 V. It was possible that these species could also plate onto the cathode. Chances however were very slim that they will interfere with the copper signal at the detector after it was solvated by the nitric acid solution. The interferences involving the electrodialysis process can be divided into two different categories, namely, the interferences of cations that may alter the flux of Cu^{2+} across the membrane due to competition and also chemical interference on the Cu^{2+} itself. These competitive interferences were evaluated by preparing the copper solutions in different brine solutions of known concentrations. It was found that at relatively low brine concentrations (ionic strength 20-200 mg ℓ^{-1}) there was no change in the sensitivity of the system or the peak profile. At concentrations of 100-10 000 mg ℓ^{-1}, there was some change in the peak profile, but no change in the total peak area. At concentrations above 10 000 mg ℓ^{-1}, the peak profiles became very uneven and the precision decreased. High concentrations of zinc ions in the samples interfered with the AAS detector. This interference was, however, circumvented by using a lean (oxidising) air-acetylene or a dinitrogen oxide-acetylene flame.

5.3.6 Data and calibration of the optimised system

The optimised parameters for the proposed electrodialysis-FI-AAS analyser for the determination of copper(II) ions in multivitamin tablets were as follows: donor flow rate, 0.32 mℓ min^{-1}; applied dc potential, 15 V; and injection loop volume, 80 $\mu\ell$.

The performance of the proposed analyser was critically evaluated under the

optimum conditions. The calibration graph was linear between 1 and 60 mg ℓ^{-1} with a relationship between peak area and copper(II) ion concentration given by the following equation:

$$y = 1.373x - 10.93 \qquad 5.1$$

where y is peak area and x is copper(II) ion concentration in mg ℓ^{-1}.

A linear regression coefficient (r^2) of 0.9975 (n = 11) was obtained over this concentration range. The percentage electrodialysis was found to be 94%. (Percentage dialysis was calculated by subtracting the percentage loss from the donor channel, when electrodialysis took place, from 100 %) The number of runs per hour for the proposed system was 14. The detection limit was calculated to be 1.44 mg ℓ^{-1}, and the sample interaction as 0.058%. (The purpose of sample interaction is to determine whether sample contamination takes place between successive samples. This is evaluated by doing the first determination with a low concentration of sample, followed by a sample with a 10 times larger concentration and then again followed by a sample containing the same amount of sample as the first). The detection limit and the sample interaction was calculated by using the following two equations:

$$\text{Detection limit} = \frac{3(S_b + I_b) - k}{m} \qquad 5.2$$

S_b: is the standard deviation of the background signal

I_b: is the relative peak area of the background signal

k: is the intercept of the calibration curve

m: is the slope of the calibration curve

$$\text{Interaction} = \left(\frac{A_3 - A_1}{A_2}\right) \times 100 \qquad 5.3$$

A_1: is the true peak area of the sample with low analyte concentration, or in

other words, the peak area obtained from a stable background.

A_2: is the true peak area of sample containing ten times more analyte than in A_1

A_3: is the peak area for the sample which will indicate the interaction with sample A_2. The concentration of A_1 is equal to A_3.

The mass of copper plated on the cathode, with a sample concentration of 20 mg ℓ^{-1}, was calculated to be 1.53 x 10^{-6} g, taking the percentage electrodialysis into account. The percentage electrodialysis was obtained by connecting the donor channel to the detector. Firstly the peak area was obtained when no dialysis or electrodialysis could take place (the acceptor channel was emptied beforehand). Hereafter the peak area was obtained from the donor channel after electrodialysis took place. The two peak areas obtained were then compared. The calculation of the percentage dialysis was done at optimised conditions.

5.3.7 Samples

The proposed system was applied to the determination of copper in a multivitamin and mineral supplement tablet. Tablets were dissolved in water and diluted to 100 mℓ. The need for membrane cleanup of the sample was illustrated once again due to the fact that the tables did not dissolve completely. Residues from the tablets could have block the nebulizer unit of the FAAS. The samples were analysed with the proposed electrodialyser-FI-AAS system by injecting them directly into the donor stream. The accuracy of the proposed system was evaluated by comparing the results obtained with those obtained by using a standard AAS procedure. In the standard method the samples were filtered manually before analysis. The results, as shown in table 5.1, revealed an excellent agreement between the two methods.

Table 5.1 Comparison of samples analysed by the proposed system and a standard AAS method

Sample	FAAS method mg ℓ^{-1}	Electrodialysis method	%RSD Proposed method
1	16.4	15.6	4.4
2	16.5	16.1	4.3
3	16.9	16.1	4.5
4	16.9	16.2	4.2
5	17.3	16.4	4.4

5.4 Conclusions

In chapter 4, it was found that the percentage dialysis of the analyte improved to a maximum of 37% (the chloride system). In this new proposed system, (the copper system) the percentage dialysis increased to a massive 94%. It was thus clear that the problems of the formation of gaseous products in the acceptor channel did not hamper the detection in this new system. The reasons for this is the following:

a: The detector used, the FAAS, was not as sensitive towards the formation of bubbles in the acceptor channel as was the case with the UV/Vis spectrophotometer.

b: In the newly developed copper method, the analyte could be plated onto the electrode in the acceptor channel which was not the case in chapter 4 with the chloride method. Due to the plating of the copper, the gas bubbles which did form, could be removed by rinsing the acceptor channel with de-ionised water before the HNO_3 was drawn into the acceptor channel for the solvation of the plated copper.

It was further possible, with larger injection volumes to preconcentrate the analyte even more and thus lower the detection limit. It would not be recommended to lower the flow rate or to increase the applied dc potential since the percentage dialysis is already 94%.

This system can also be applied for the analysis of very low concentrations of copper. In the preposed system, the use of the electroplating of the copper ions was not exploited to its full capacity. By increasing the injection volume, very low copper concentrations can be injected and copper trace enrichment can take place in the acceptor channel.

As is evident from the fact that the acceptor channel could be rinsed (to remove all the gaseous products formed at the cathode) before the copper was to be solvated in the HNO_3, this ED/FIA system can also be used with ease with detectors that are very sensitive towards the presence of bubbles (gaseous products in the acceptor channel) in the flow system. Also it will be possible to use an electrochemical detection system since the ED can switched off before the solvation and analysis of the Cu^{2+} ions.

The massive increase of the percentage dialysis from the chloride system to the copper system is mostly due to the much lower flow rate in the donor channel of the copper system. (2.0 mℓ min^{-1} in the chloride system to 0.32 mℓ min^{-1} in the copper system) It is further possible that the migration rate of the copper ions under the influence of an applied potential is higher for the copper ions than for the chloride ions. A possible explanation for this that the chloride ions may be more hydrated in solution than is the case with the copper ions. When this happens, the effective radius of the chloride ion will be much larger than that of the copper ion (both ions in solution). This enlarged effective radius of the chloride ions in solution will then in turn give rise to a lower drift speed of the chloride ions under in influence of the applied dc potential. (See paragraph 3.1)

The proposed electrodialyser-FI-AAS system is suitable for the analysis of samples containing solid particles in suspension. These particles were of such a nature that they continuously blocked the inlet path to the nebulizer of the AAS detector. The flexibility of the electrodialyser-FI system is not only the removal of the solid particles from the analyte, but also retaining the analyte concentration in an acceptor channel the same as it was originally in the donor channel.

5.5 References

1 Burguera, J.L., (**1989**) Flow Injection Atomic Spectroscopy, Marcel Dekker, New York.

2. Kuban V., Komarek J., Cajkova D., (**1989**) Collect. Czech. Chem. Commun. 54(10): 2683.

3. Hirata S., Honda K., Kumamaru T., (**1989**) Anal. Chim. Acta. 221(1): 65.

4. Purohit R., Devi S., (**1991**) Talanta. 38(7): 753.

5. Carbonell V., Mauri A.R., Salvador A., De La Guardia M., (**1991**) J. Anal. At. Spectrom. 6(7): 581.

6. Burguera J.L., Burguera M., Matousek de Abel de la Cruz A., Anez N., Alarcon O.M., (**1992**) At Sectrosc. 13(2): 67.

7. Naghmush A.M., Trojanowicz M., Olbrych-Sleszynska E., (**1992**) J. Anal. At. Spectrom. 7(2): 323.

8. Ma R., Van Mol W., Adams F., (**1994**) Anal. Chim. Acta. 285(1): 33.

9. Elmahadi H.A.M., Greenway G.M., (**1994**) J. Anal. At. Spectrom. 9(4): 547.

10. Maquieira A., Elmahadi H.A.M., Puchades R., (**1994**) Anal. Chem. 66(9): 1462.

11. Maquieira A., Elmahadi H.A.M., Puchades R., (**1994**) Anal. Chem. 66(21): 3632.

12. Burguera J.L., Burguera M., Carrero P., Marcano J., Rivas C., Brunetto M.R., (**!995**) J. Autom. Chem. 17(1): 25.

13. Van Staden J.F., Hattingh C.J., (**1995**) Anal. Chim. Acta. 308(1-3): 214.

14. Van Staden J.F., Hattingh C.J., (**1995**) J. Anal. At. Spectrom. 10(10): 727.

15. Ma R., Van Mol W., Adams F., (**1996**) At. Spectrosc. 17(4): 176.

16. Zhuang Z.X., Wang X.R., Yang P.Y., Huang B.L., (**1994**) Can. J. Appl. Spectrosc. 39(4): 101.

17. Azeredo L.C., Sturgeon R.E., Curtius R.J., (**1993**) Spectrochim. Acta. 48B(1): 91.

18. Ebdon L., Fisher A.S., Worsfold P.J., Crews H., Baxter M., (**1993**) J. Anal. At. Spectrom. 8(5):691.

19. Yang C.L., Zhuang Z.X., Wang X.R., Quin S.D., Yang P.Y., (**1994**) At. Spectrosc. 15(3) 135.

20. Bortoli A., Gerotto M., Marchiori M., Mariconti F., Polonta M., Troncon A., Microchem. J. 54(4): 402.
21. Hwang T., Jiang S.J., (**1996**) J. Anal. At. Spectrom. 11(5): 353.
22. Izquierdo A., Luque de Castro M.D., Valcarcel M., J. (**1993**) Autom. Chem. 15(4): 121.
23. Matysik F.M., Gerner G., (**1993**) Analyst. 118(12): 1523.
24. Izquierdo A., Luque de Castro M.D., Valcarcel M., J. (**1994**) Electroanalysis. 6(10): 894.
25. Chow C.W.K., Kolev S.D., Davey D.E., Mulcahy D.E., (**1996**) Anal. Chim. Acta. 330(1): 79.
26. Haj Hussein A.T., (**1996**) Talanta. 43(11): 1909.
27. Hattingh C.J., (**1994**) MSc. dissertation, University of Pretoria.
28. Chimpalee N., Chimpalee D., Srithawepoon S., Patjarut T., Thorburn Burns D., (**1995**) Anal. Chim. Acta. 304(1): 97.
29. Liu R.M. Liu D.J., Sun A.L., (**1993**) Talanta. 40(4): 511.
30. Barnes D.E., Jones E.A., (**1989**) Mintek report nr. M389. Council for mineral Technology.
31. Szpunar Lobinska J., Trojanowicz M., (**1990**) Anal. Sci. 6(3): 415.
32. Maquieira A., Elmahadi H.A.M., Puchades R., (**1996**) Analyst. 121(11): 1633.
33. Esmadi F.T., Khasawneh I.M., Kharoaf M.M., Attiyat A.S., (**1992**) Can. J. Appl. Spectrosc. 37(5): 119.
34. Cox J.A., Twardoski Z., (**1980**) Z. Anal. Chim. Acta. 119: 39.
35. Cox J.A., Carnahan J.W., (**1981**) Appl. Spectrosc. 35: 447.
36. Cox J.A., Dabek-Zlotorzynska E., Saari, R., and Tanaka, N., (**1988**) Analyst. 113: 1401.
37. Koropchak J.A., Allen L., (**1989**) Anal. Chem. 61: 1410.
38. Kasthurikrishnan, N., Koropchak J.A., (**1993**) Anal. Chem. 65: 857.
39. Kuban V., Komarek J., Chajkova D., (**1989**) Collect. Czech. Chem. Commun. 54: 2683.
40. Carbonell V., Salvador A., De la Guardia M., (**1992**) Fresenius' J. Anal. Chem.

324: 529.

41. Turnell D.C., Cooper J.D.H., (**1985**) Autom. Chem., 7: 177.
42. Turnell D.C., Cooper J.D.H., (**1985**) Autom. Chem. 7: 181.
43. Cox J.A., Carlson R., (**1981**) Anal. Chim. Acta. 130: 313.
44. Van Staden J.F., Hattingh C.J., unpublished work.
45. Van Staden J.F., Van Rensburg, A., (**1990**) Analyst. 115: 1049.
46. Marshall, G.D., Van Staden, J.F., (**1992**) Anal. Instrum.. 20: 79.
47. Schoeman, J.J., (**1992**) PhD Thesis, University of Pretoria.
48. Schoeman, J.J., Van Staden, J.F., (**1991**) Water SA, 1991, 17: 307.
49. Schoeman, J.J., Van Staden, J.F., (**1997**) J. Membr. Sci. 132: 1.

Chapter 6

Determination of zinc in pharmaceutical products using an electrodialyser incorporated into a flow injection system.

6.1 Introduction

The first studies linking zinc and growth were done in Iran and Egypt almost 3 decades ago. Zinc, as a trace mineral, is of utmost importance for normal human bodily functions. Minerals and vitamins are essential components of the diet. The body cannot synthesize minerals and the cells can generate only a small quantities of very few vitamins. [1] Minerals are inorganic ions released through the dissociation of electrolytes. Zinc is a trace mineral in the human body with a total body content of an adult human of 2 - 3 g. The highest concentrations are in the liver, kidneys, pancreas, bone, voluntary muscle, parts of the eyes, prostate gland, spermatozoa, skin and nails. [1,2] Zinc is known to participate in reactions involving either the syntheses or degradation of major metabolites such as carbohydrates, lipids, proteins and nucleic acids. More than 200 zinc enzymes have been isolated from different species. Zinc is also involved in the stabilization of protein and nucleic acid structure and the integrity of subcellular organelles and transport processes, immune function and expression of genetic information. Zinc acts as a cofactor of enzyme systems, notably carbonic anhydrase. Zinc deficiency can cause delayed wound healing, alopecia and diverse forms of skin lesions. [1, 2]

Atomic spectroscopy is one of the most sophisticated and elegant methods for direct assay of cations. [3,4] Atomic absorption spectrometry (AAS) allows no fewer than 70 metals to be determined directly, which makes it very suitable for many clinical and forensic analysis. Furthermore, indirect AAS methods allow many techniques to be extended to the analysis of a number of analytes besides metals (including anions and organic compounds). [5] Suspended solids, macromolecules and high salt

concentrations in samples, however, caused nebulizer clogging and ultimately blocked the nebulizer. This resulted in inaccurate results and low precision. To avoid this the nebulizer had to be removed and cleaned frequently, but the analysing process then became tedious and time consuming.

AAS in association with flow injection (FI) analysis is considered a very competent method for pharmaceutical sample analysis. The advantages of the FI-AAS association is matrix removal and analyte preconcentration. [5] Various means of matrix removal are possible in chemical analysis. According to Debrah *et al.* [6], precipitation is the oldest method of chemical separation. Precipitation methods are satisfactory for macro separations, although precipitates are usually contaminated with foreign ions present in the solution. Precipitation is useful to remove a major constituent of a sample if this constituent interferes with the subsequent determination of trace components. In an FI system it is possible to retain small quantities of precipitate on an in-line filter. It is even possible to retain the analyte element co-precipitated on the interior of an open knotted tube reactor. It is however not possible to use an in-line filter in an FI system for large amounts of precipitates. To overcome this problem, the use of a recirculating, closed-loop manifold for sample pretreatment was described by Debrah *et al.* [6] Solvent extraction is another very successful method of matrix removal. When analysing zinc (at the 213.856 nm line), a large excess of iron can interfere, originating from the weak 213.859 nm iron line. Removal of the iron interference by means of solvent extraction was done by Sweileh and Cantwell.[7] Similar work and the influence of a masking agent was illustrated by Ma *et al.* [8] The use of an ion-exchanger (eg. Chelex 100) has also been used extensively not only as a method for preconcentration, but also as a means to separate matrix interferences.[9] An alternative approach is to immobilise a micro-organism cell wall on an insoluble substrate. Living organisms have the ability to absorb trace metals from an aqueous solution.[10]

The problem of nebulizer clogging by high salt concentrations is not so severe when the AAS is interfaced to an FI system, but this is not the ultimate solution. Although the carryover is small, a gradual drop in the sensitivity was observed by Davey [11] when

analysing samples with high salt concentrations. The use of neutral dialysis membranes (passive dialysis) in flow-through dialysers as part of FI systems is an extremely powerful tool to remove suspended solids and macromolecules in order to let the analyte flow unhindered to the detector. Unlike filter systems, the part of the sample matrix containing suspended solids is continuously channelled via the donor stream to waste, while the clear dialysed analyte solution in the acceptor stream is flushed to the detector.

We successfully incorporated passive neutral membranes as part of various FI systems in our laboratory to remove interferences, before the determination of analytes. [12 - 18] We also included an electrodialyser (fitted with a passive neutral membrane) successfully as part of FI-AAS systems to enhance mass transfer together with the removal of interferences. [17, 18] A similar approach was used by Buschner *et al.* [19] during the on-line analysis of adenosine triphosphate and inositol phosphate with electrodialysis-capillary zone electrophoresis.

The main objective of this project was to develop a method that will be able to handle samples with high salt concentrations and at the same time remove the matrix interferences during the determination of zinc in pharmaceutical products.

6.2 Experimental

6.2.1 Reagents and Standards

All glassware and storage bottles were soaked in 10 % (v/v) nitric acid overnight and rinsed with de-ionised water prior to use. All reagents were of analytical grade and de-ionised water, obtained from a Modulab water system, was used for the preparation of all stock solutions and dilutions of standards. A 1000 mg ℓ^{-1} zinc(II) stock solution was prepared by dissolving 1.000 g zinc granules in 40 mℓ 1:1 hydrochloric acid, and dilute it to the mark in a 1ℓ volumetric flask. Electrolyte stock solution was prepared by dissolving 25.42 g of sodium chloride in a 1 ℓ volumetric flask and made up to the mark with de-ionised water. Suitable dilutions

of the stock solutions were made to prepare the zinc standards. The percentage nitric acid in the standard zinc solutions was also adjusted to be 1% (v/v) and the electrolyte concentration in all the zinc solutions was 0.31 mol ℓ^{-1} in sodium. Standard solutions were prepared daily. [20] The rinsing solution consisted of a 1 % (v/v) nitric acid solution and a 0.31 mol ℓ^{-1} sodium solution. (Sodium solution prepared from dried sodium chloride)

6.2.2 Instrumentation

The FI system (Figure 6.1) used was composed of the following components:

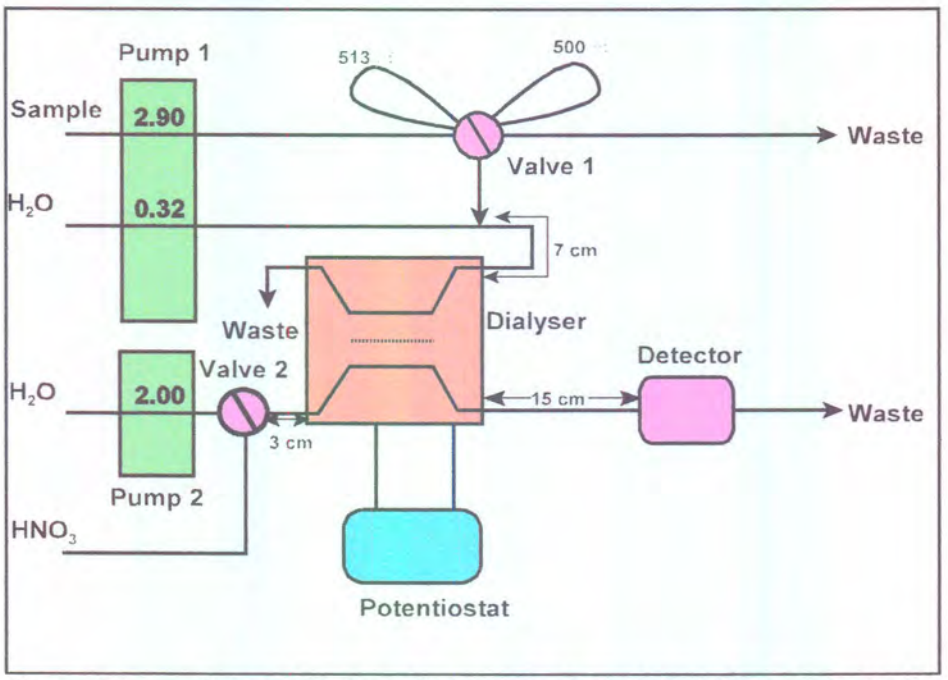

Figure 6.1 Schematic flow diagram of the ED-FI-AAS system for the determination of zinc.

1. A six-roller Cenco peristaltic pump (rotating at 10 rev min^{-1})
2. One Valco 10-port electrically actuated injection valve (Houston, TX, USA). The injection valve was configureured in such a way that it consisted of a sample loop of 513 $\mu\ell$ and a rinsing loop of 500 $\mu\ell$. These two loops were used to alternating inject the sample solution and the rinsing solution into the donor carrier stream of the electrodialyser (see

Figure 6.2).

3. The manifold consisted of Tygon tubing, with an internal diameter (id) of 0.76 mm, cut the required lengths and wound around Perspex rods with an outer diameter (od) of 10 mm. The electrodialyser unit used (Figure 6.2) was a slightly modified version of the dialyser previously described by van Staden and van Rensburg [12] It is similar to the one used in chapter 4 for the determination of chloride with the only difference that the polarity on the electrodes were swopped so that the anode was situated in the donor channel and the cathode in the acceptor channel. The dialyser unit consisted of two, mirror image, PVC blocks. Embedded into each of these blocks were graphite electrodes which acted as the anode (acceptor side) and the cathode (donor side) respectively. Placed onto each of the PVC blocks was a 0.6 mm thick Perspex spacer. Into each of the Perspex spacers, a groove of 0.6 mm diameter and 300 mm length was cut so as to form a channel when placed onto each of the PVC blocks respectively. The PVC blocks were then fitted onto each other in such a way that the Perspex spacers facing each other and the grooves in the respective Perspex blades coincided with each other. The membrane was then sandwiched between the two Perspex spacers as the only separation between the two tubes so formed. The walls of the tubes that were formed thus consisted of, at the far end, the graphite (which was embedded into the PVC blocks), the side walls of Perspex and the common wall, the membrane. A Technicon pre-mount membrane was used in the dialyser unit.
4. A Leader LPS 156 potentiostat was used to apply the dc potential.
5. A Prema 5000 integrating multimeter was used for current and potential measurements.
6. A Varian AA 1275 Atomic absorption spectrometer (Palo Alto, CA, USA) was used as the detector. A Varian Techtron Zn hollow cathode lamp, with a current of 7 mA, was used to give a monochromatic light ray in the detector. A wavelength of 213.9 nm and a spectral bandpass of 0.2 mm

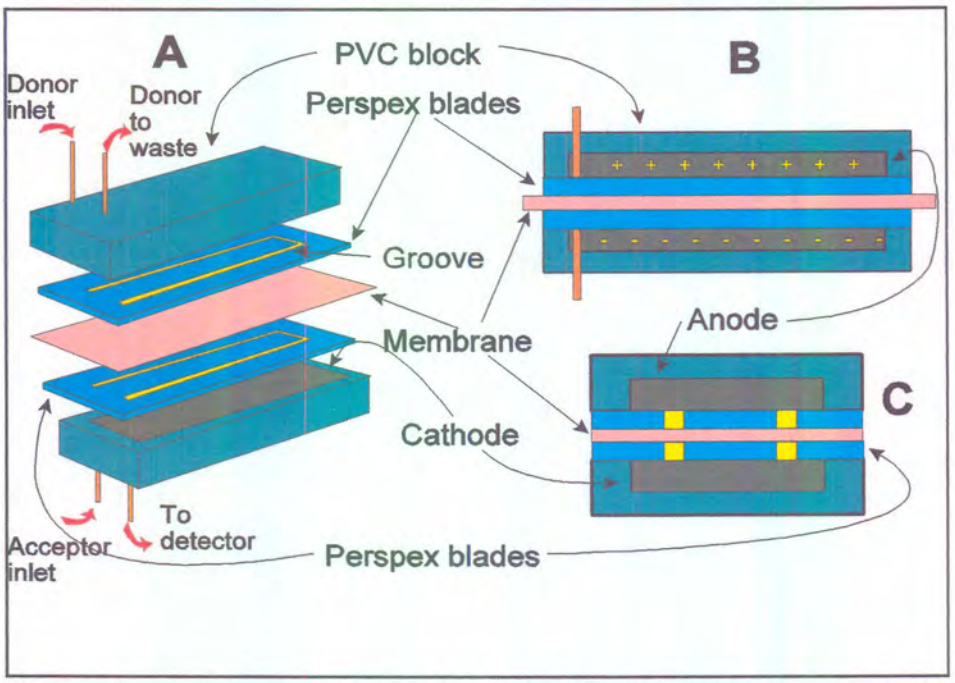

Figure 6.2 *Schematic presentation of the Electrodialyser unit. A - the 3D presentation, B - a longitudinal cross-section and C - a diagonal cross-section.*

was used. A lean (oxidising) air/acetylene flame was used.

7. The AAS detector, pump and valve were coupled to a personal computer equipped with the *FlowTEK* program. [21]

6.2.3 Flow system and Procedure

A single run consisted of the following procedures: (See Figure 6.3 for the timing diagram)

Operation of pump and valve

A timing diagram for the FI-AAS system is depicted in Figure. 6.3. The pump was never switched off during the analysis. The valve was switched between the "load" and the "inject" position. During the "load" position, the 513 $\mu\ell$ loop was filled with a sample, whilst the 500 $\mu\ell$ was connected to the donor channel. When

the valve was switched to the "inject" position, the 513 $\mu\ell$ loop was connected to the donor channel (thus injecting the sample into the donor channel), whilst the 500 $\mu\ell$ was filled with the rinsing solution.

The system was switched on and allowed to run for about 5 minutes in order to equilibrate the flow dynamics of all parts of the system. The computer was then actuated and the timing sequence started in the load position.

(i) Starting the system. (Loading)

Pump: The pump was switched on. Flow rates in the donor and acceptor channels were both 1.40 $m\ell\ min^{-1}$. The inlet tubing, connected to the donor channel, was removed from the water container so that air was pumped through the donor channel and de-ionized water was pumped through the acceptor channel.

Valve: The valve was switched to the load position. In the load position the 500 $\mu\ell$ loop was connected to the donor channel and the 513 $\mu\ell$ loop was filled with sample solution.

Potentiostat: The potentiostat was set to on position at 17.5 V.

(ii) Analysis

At time T = 0 s, the valve was switched to the "inject" position, thus

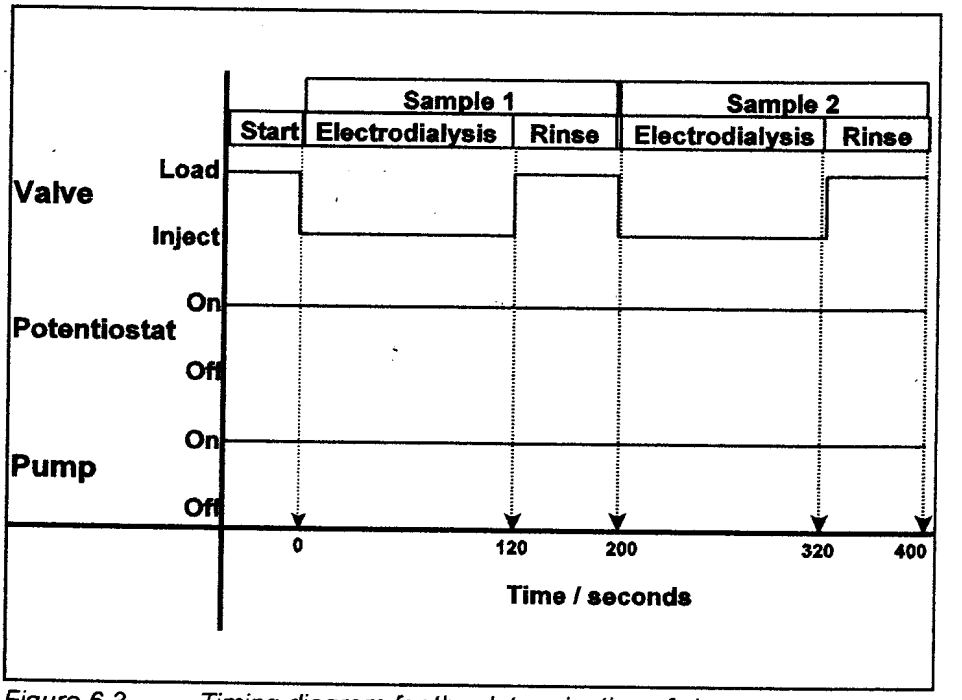

Figure 6.3 *Timing diagram for the determination of zinc*

directing the 513 $\mu\ell$ loop to the donor channel, whilst the 500 $\mu\ell$ loop was filled with rinsing solution. The sample plug was pumped through the donor channel at a rate of 1.40 mℓ min^{-1}. The applied potential over the membrane was kept constant at 17.5 V for the duration of the electrodialysis step. Analyte ions in the sample plug electrodialysed through the membrane into the acceptor channel. These analyte ions were then transported via the acceptor channel to the detector. At time T = 120 s, the valve was switched to the "load" position again to fill the 513 $\mu\ell$ loop for the next run and at the same time directing the 500 $\mu\ell$ rinsing solution into the donor channel.

Data acquisition and device control were achieved using a PC30-B interface board (Eagle Electric, Cape Town, South Africa) and an assembled distribution board (MINTEK, Randburg, South Africa). The *FlowTEK*[16,21] software package (obtainable from MINTEK) for computer-aided flow analysis was used throughout

for device control and data acquisition. All the data given (mean peak area values) are the average of 11 repetitions.

6.3 Results and discussion

In previous work done by van Staden and Hattingh [18], a similar approach was used for the analysis of copper(II). The zinc and the copper systems differ in the sense that in the latter system, copper metal was plated onto the cathode in the stagnant acceptor channel. It was however not possible to apply this procedure for the zinc determination since the reduction potential of zinc, at standard conditions, is much lower than 0 V The objective of this study was to introduce a zinc analyte plug from the FI system into the detector which was free from possible matrix interferences, but still have a high enough concentration so that preconcentration will not be necessary. To obtain this goal, it was imperative to ensure that the mass transfer across the membrane during the electrodialysing step was as high as possible (Figure 6.2). One of the disadvantages of a dialysis system is the fact that the dialyser has a double dilution effect on the analyte. Firstly, in the form of a massive increase in the dispersion of the analyte sample plug whilst passing through the dialyser and secondly, in the case of passive dialysis without the application of the electrical field across the membrane, the percentage dialysis varies between 0-7%. [16] Prevention of the dispersion in the donor channel was achieved by making use of air as the carrier (instead of de-ionised water). In the acceptor channel de-ionised water was pumped through continuously.

The FI-AAS system was optimised, according to achieved sensitivity and reproducibility, under the following headings:

6.3.1 Applied potential across the membrane

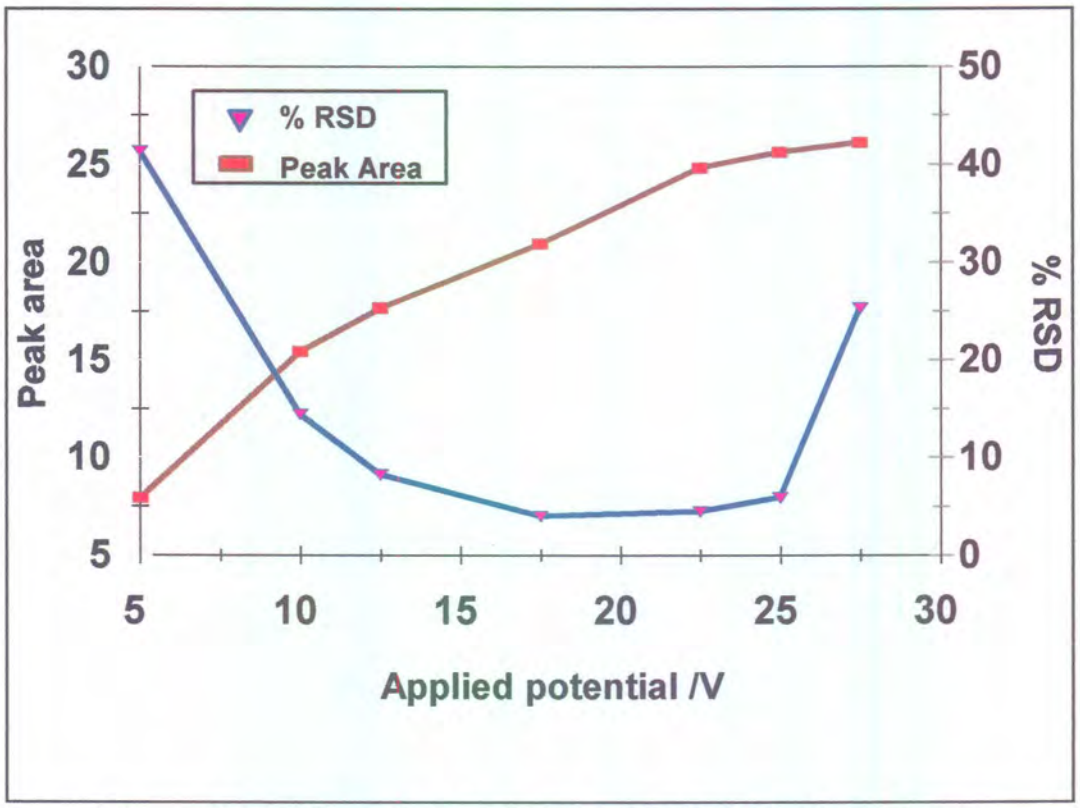

Figure 6.4 Effect of the applied dc potential on the % RSD and the peak area

Of all the parameters optimised (flow rate of the donor and acceptor streams, injection loop volume and electrolyte concentration), the applied potential had the largest influence on the migration rate of zinc ions across the membrane. The influence of the applied potential on the average peak area is illustrated in Figure 6.4. The flow rates of the donor- and acceptor channels were kept constant at 1.40 mℓ min^{-1} during the optimisation of the applied potential. It is clear from Figure 6.4 that the optimum potential in both the average peak area and the % RSD lies between 17.5 and 22.5 V. The optimum applied potential with the better sensitivity is at 22.5 V (Figure 6.4) with the reproducibility more or less the same. What is however not indicated on the graph in Figure 6.4 is the massive peak distortions which occurred at 22.5 V and to a much lesser extent at 17.5 V. These distortions were the result of gas formation at the cathode in the

acceptor channel. It is possible that these peak distortions can alter the analysis of real samples which may contain species that have high gas formation capabilities. It is clear that rather high RSD values occurred at the extremes of the measured applied potentials. At the higher potential (27.5 V), there was a very high rate of gas formation (and thus also a distortion of the peak) which in turn led to the higher RSD values. At the low applied voltages, the migration rate of the zinc across the membrane was so low that the reproducibility was increasingly influenced by the noise of the instrument. From Figure 6.5 it is evident that there is nearly a linear relationship between the applied dc potential and the electrical current across the membrane. It can be assumed that there will be a further increase in the current with increasing applied dc potential, but due to increased RSD values at higher applied potentials (see Figure 6.4), it was not recommended. The potential of 17.5 V was therefore chosen as the optimum applied potential.

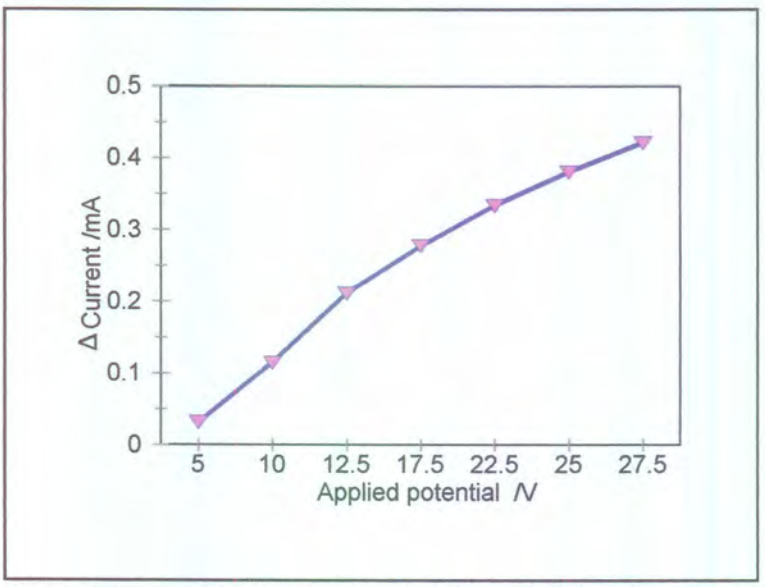

Figure 6.5 *Effect of the applied dc potential on the change of current in tie acceptor channel indicating the flux of ions through the passive neutral membrane*

6.3.2 Flow rates of the donor and the acceptor streams

The flow rates in the donor and the acceptor channels had the next largest influence on the diffusion rate of the analyte across the membrane. The flow rates of the donor and the acceptor streams were kept the same throughout the optimisation. Optimisation was done by injecting 10.0 mg ℓ^{-1} Zn^{2+} into the donor channel and keeping the applied potential across the membrane constant at 17.5 V. As can be seen from Figure 6.6, there was a steady decrease in the average peak area with the increase in the flow rate of the donor and the acceptor channels. The optimum flow rate was taken between 1.4 and 2 mℓ min^{-1}. At these flow rates the % RSD was also at its lowest. Too high flow rates prevented the transfer of the bulk of the zinc ions across the membrane to the acceptor channel, whereas too low flow rates led to unnecessary high analysis times.

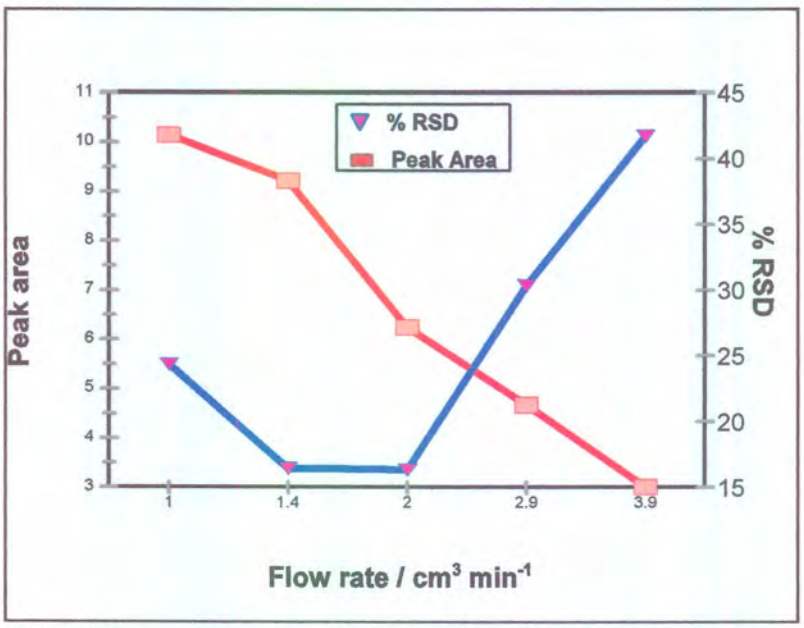

Figure 6.6 *Influence of the flow rate of the donor- and acceptor stream on the % RSD and the peak area.*

6.3.3 Injection loop volume

The flow rates of the donor and the acceptor streams were kept constant at 1.4 mℓ min^{-1} and the applied potential at 17.5 V during the optimisation of the injector loop volume. It can be seen from Figure 6.7 that there is a linear increase in the average peak area with increasing injection loop volume. The % RSD was rather low at most of the injection loop volumes with a slight elevation at the smaller injection loop volumes. The optimum injection loop volume was taken to be 513 $\mu\ell$. Even though larger injection loop volumes gave higher average peak areas with not much change in the % RSD, the higher injection loop volumes resulted in much longer experimental times and a lower throughput of samples.

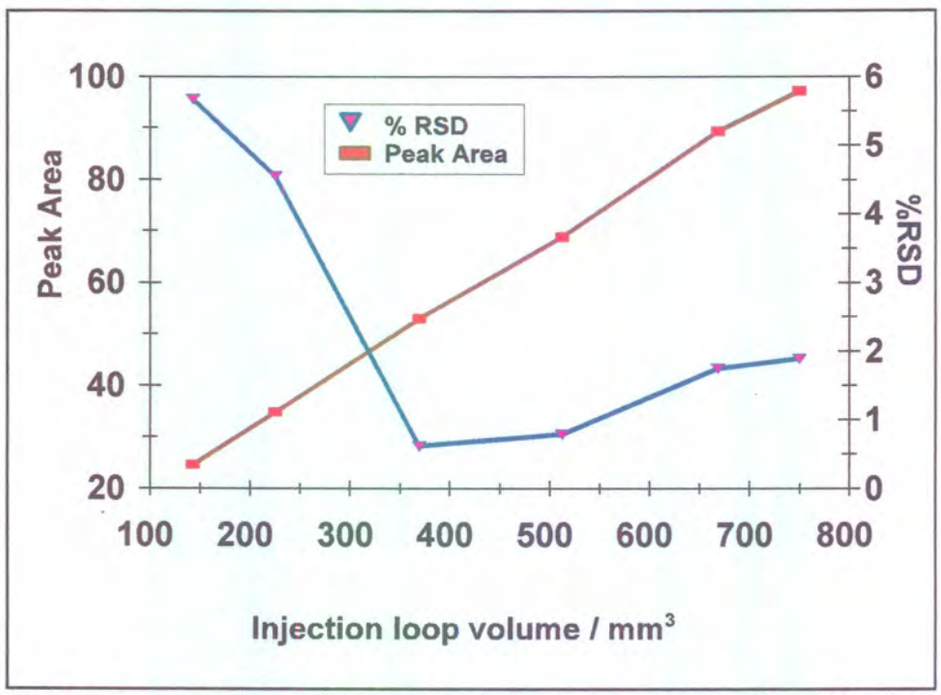

Figure 6.7 *Influence of the injection loop volume on the % RSD and the peak area*

6.3.4 Addition of an electrolyte

The migration rate of ions under the influence of an applied potential is altered by the addition of an electrolyte. With the addition of an electrolyte, the hydration of the analyte ion is changed and therefore also the effective ion radius of the ion in motion (the analyte). [22]. In addition to this, it was found that there was a slight retention of the analyte on the membrane. (After rinsing the donor channel with an electrolyte solution, traces of the analyte was found in the acceptor channel) To address both these situations, an electrolyte was added to all the solutions that were analysed. There was an increase in the zinc signal with the addition of the electrolyte. This phenomenon indicated that the migration of zinc across the membrane was enhanced with the addition of the electrolyte. The electrolyte concentration was increased up to the point where an increase in the electrolyte concentration did not further enhance (or alter) the zinc signal. An electrolyte solution (without zinc analyte) was used to rinse the dialyser between two consecutive runs to ensure that all the analyte ions were removed from the dialyser and the membrane. Sodium chloride at a concentration of 0.31 mol ℓ^{-1}, was used as the electrolyte. The counter anion, however, did not have an influence on the migration of zinc(II) ions across the membrane as long as it is neutral, but an anion with basic properties led to the precipitation of the zinc(II) ions.

6.3.5 Interferences

The electrodialyser was found to be an excellent means of sample cleanup. It is known that iron(III) can interfere with the 213.9 nm Zn line. The influence of iron(III) on the zinc analysis is depicted in Figure 6.8. It is clear from Figure 6.8 that iron in concentrations above 7.5 times the zinc concentration in the sample seriously altered the zinc signal. Masking agents like oxalate, phosphate, citrate, tartrate and fluoride can be used to eliminate the iron(III) interference. The use of these masking agents during the extraction of zinc was studied by Ma *et al.* [8]

Some of these masking agents had a negative influence on the zinc signal. The addition of fluoride ion to the zinc/iron mixture decreased the effect of the iron(III) to such an extent that the system could tolerate iron(III) concentrations up to ten times the zinc concentration in the samples before any alterations in the zinc signal was observed. Since all the fluoride ions migrated to the anode, the excess fluoride ions were perfectly removed from the zinc, which migrated across the membrane towards the cathode. It was thus possible to add a large excess of the masking anions without interferences with the zinc determination. It is thus clear that any anion or neutral species which interferes with the zinc can easily be separated from the zinc before analysis.

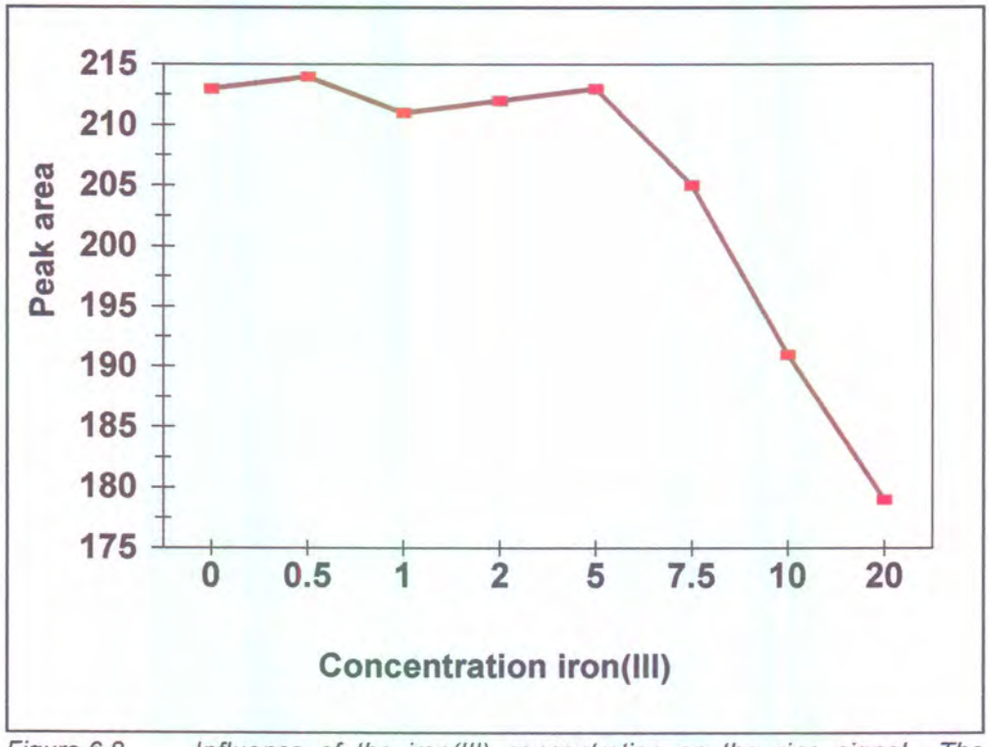

Figure 6.8 *Influence of the iron(III) concentration on the zinc signal. The concentration of the iron(III) is given as a multiple of the zinc concentration*

Anionic or neutral zinc complex formation would severely interfere with the analysis of zinc(II) ions. To prevent complex formation or to destroy any possible

zinc complexes, low pH's were maintained in all working solutions. In a strong acidic medium most of the zinc complexes will be destroyed. Apart from the simulated gastric fluid, nitric acid was added to the solutions so that the pH was < 1.0.

6.3.6 Data and calibration of the optimised system

The optimised parameters for the proposed electrodialysis-FI-AAS analyser for the determination of zinc(II) ions in multivitamin tablets are as follows:

Donor and acceptor flow rate:	1.40 mℓ min^{-1}
Applied potential:	17.5 V
Injection loop volume:	513 $\mu\ell$

The performance of the proposed analyser was critically evaluated under the optimum conditions. The calibration graph was linear between 1 and 20 mg ℓ^{-1} with the relationship between peak area and zinc(II) ion concentration given by the the following equation:

$$y = 7.14x + 12.17, \qquad 6.1$$

where y = peak area and x = zinc(II) concentration in mg ℓ^{-1}. A linear regression coefficient (r^2) of 0.9972 with n = 11 was obtained over this concentration range. The number of runs per hour for the proposed system was 18. The detection limit was calculated to be 0.998 mg ℓ^{-1} and the sample interaction as 0.0015 %. The detection limit and the sample interaction was calculated by using the following two equations:

$$\text{Detection limit} = \frac{3(S_b + I_b) - k}{m} \qquad 6.2$$

S_b: is the standard deviation of the background signal

I_b: is the relative peak area of the background signal

k: is the intercept of the calibration curve

m: is the slope of the calibration curve

$$\text{Interaction} = \left(\frac{A_3 - A_1}{A_2}\right) \times 100 \qquad 6.3$$

A_1: is the true peak area of the sample with low analyte concentration, or in other words, the peak area obtained from a stable background.

A_2: is the true peak area of sample containing ten times more analyte than in A_1

A_3: is the peak area for the interacted sample containing the same concentration of analyte as A_1

6.3.7 Samples

Multivitamin tablets were obtained from a local drug store. Three different tablets, referred to as follows, were analysed.

Sample tablet ST 1:	Vital Zinc
Sample tablet ST 2:	Extravite multivitamin tablets
Sample tablet ST 3:	Weigh less multivitamin tablets

All the sample tablets were dissolved in de-ionised water after which a simulated gastric fluid was added according to the United States Pharmacopeia guidelines. [23] After dissolution in the simulated gastric fluid, care was taken that the pH of the solutions was kept low during the dilutions of the samples. This was achieved by adding nitric acid in order to keep the acid concentration in the 1% (v/v) range. (Even though the simulated gastric fluid has a pH of about 1.2, it has no buffering capabilities leading to a pH increase with the dilution of the sample. It was further necessary to obtain a low pH so that all possible zinc complexes were destroyed). During the dilution of the sample, care was taken that the final sodium

concentration in the sample was at least 0.31 mol ℓ^{-1}. The accuracy of the proposed system was evaluated by comparing the results with those obtained using a standard AAS procedure. It is worthwhile to note that the samples used for the standard AAS method had to be filtered before analysis, since not all the constituents of the tablets were soluble. (We had great difficulties in cleaning the volumetric flasks in which the samples were prepared but no clogging of the dialyser unit or FIA system were observed. Nebulizer clogging would have occurred if the sample wasn't dialysed, since the grooves in the dialyser unit were considerably larger than that of the nebulizer.) The results, as shown in Table 6.1, revealed an excellent agreement between the two methods. The results were also in close agreement with the distributers note.

Table 6.1 *Comparison of the results of samples analysed by the proposed system, a standard AAS method and the distributors note. All concentrations are given in mg ℓ^{-1}. The subscript at each tablet's name indicate that three tablets of each kind were analysed*

Sample nr.	Proposed FIA/electrodialyser system	% RSD	FAAS	Distributers note
ST 1_1	14.67	2.39	14.98	15
ST 1_2	14.89	2.41	15.01	15
ST 1_3	14.77	3.09	14.07	15
ST 2_1	3.59	3.78	3.78	3.75
ST 2_2	3.80	3.85	3.67	3.75
ST 2_3	3.77	3.69	3.70	3.75
ST 3_1	7.59	3.51	7.62	7.5
ST 3_2	7.65	3.29	7.66	7.5
ST 3_3	7.55	3.44	7.60	7.5

6.4 Conclusions

The proposed FI-electrodialysis-AAS system proved itself to be a very useful tool for the removal of matrix interferences during the determination of zinc in pharmaceutical products. Iron interference was eliminated with the addition of an excess of fluoride ions and in the tablets that were analysed, where the iron concentration was very similar to that of the zinc, it did not really pose a problem during the determination of the zinc. This system can very easily be applied to the determination of zinc in practically any sample. The proposed system should be particularly attractive for pharmaceutical laboratories where solid particles, macromolecules and high salt concentrations in samples are problematic to analyse with conventional AAS instrumentation.

6.5 References

1. Martini, F. H., **(1995)** *Fundamentals of Anatomy and Physiology*, 3rd edition, Prentice-Hall.
2. Mahan, L. K., and Arlin, M. T., **(1992)** *Food, Nutrition and Diet Therapy*, 8th edition, WB Saunders Company.
3. Simonsen, K. W., Nielsen, B., Jensen, A. S., and Andersen, J. R., **(1986),** *Journal of Analytical Atomic Spectrometry*, **1**, 453.
4. Burguera, J. L., **(1989)** *Flow Injection Atomic Spectroscopy*, Marcel Dekker, New York,.
5. Sperling, M., Kościelniak, P., and Welz, B., **(1992)** *Anal. Chim. Acta.*, **261,** 115.
6. Debra, E., Tyson, J. F., and Hinds, M. W., **(1992)** *Talanta*, **39**, 1525.
7. Sweileh, J. A., and Cantwell, F. F, **(1985)** *Anal. Chem.*, **57**, 420.
8. Ma, R., Van Mol, W., Adams F., **(1995)** *Anal. Chim. Acta.*, **309**, 395.
9. Olsen, S., Pessenda, L. C. R., Růžička, J., and Hansen, E. H., **(1983)** *Analyst*, **108**, 905.
10. Maquieira, A., Elmahadi, H. A. M., and Puchades, R., **(1994)** *Anal. Chem.*, **66**, 3632.
11. Davey, D. E., **(1986)** *Anal. Lett.*,, **19**, 1537.
12. Van Staden, J. F., and van Rensburg, A., **(1990)** *Analyst*, **115,** 1049.
13. van Staden, J. F., and van Rensburg, A., **(1989)** *Fresenius Zeitschrift für Anal. Chem.*, **334,** 695.
14. van Staden, J. F., and van Rensburg, A., **(1990)** *Fresenius J. Anal. Chem.*, **337,** 393.
15. van Staden, J. F., **(1991)** *Fresenius' J. Anal. Chem.*, **340,** 415.
16. van Staden, J. F., **(1995)** *Fresenius' J. Anal. Chem.*, **352,** 271.
17. van Staden, J. F., and Hattingh, C. J., **(1998)** *Talanta*, **45**, 485.
18. van Staden, J. F., and Hattingh, C. J., **(1998)** *Journal of Analytical Atomic Spectrometry*, **13**, 23.
19. Buschner, B. A. P., Tjaden, U. R., van der Greef, J., **(1997)** *Journal of*

Chromatography A, **764**, 135.

20. von Loon, J. C., **(1982)** *Chemical Analysis of Inorganic constituents of Water,* CRC press.
21. Marshall, G. D., and van Staden, J. F., **(1992)** *Anal. Instrum.,* **20,** 79.
22. Bard, A. J., and Faulkner, L. R., **(1980)** *Electrochemical Methods, Fundamentals and Applications,* John Wiley & Sons.
23. The United States Pharmacopeia. **(1995)** The National Formulary, USP23 NF18.

Chapter 7

The determination of phosphate

7.1 Introduction

Phosphorus primary exists as phosphate in natural and water effluents. These phosphates include ortho-phosphate, condensed phosphates (pyro-, meta-, and other polyphosphates), and organically bonded phosphates. These phosphates exist in water as a solution, small particles or in living material. [1]

Ecologically phosphorus is an important compound due to the role it plays in a variety of cell processes. Phosphorus is one of the primary nutrients for normal growth of plants and animals. [2] Phosphorus in the human body consist mainly as phosphate (or orthophosphate). About 80 -85 % of the total phosphate is combined with calcium in bones and teeth. The remainder is combined with protein, lipid, carbohydrate and enzymes. Besides its structural importance in bones and teeth, phosphate also plays a major role in the absorption process of glucose and glycerol in the intestine, and in the formation of many enzymes essential to the intracellular oxidation process and production of energy. It also forms an active part of the buffer system in the body. [3,4]

Various analytical methods for the determination of orthophosphate are exploited so far in flow injection analysis. Two prominent methods made use of the reaction of phosphate with a colour reagent and measuring the coloured product with a spectrophotometer. The first of these methods was the phosphomolybdenum blue method. [5 - 12] The second was the molybdophosphate with malichite green method. [13, 14] Other methods included the use of high-performance liquid chromatography [15] and amperometric methods. [16] One other method was the indirect determination of phosphate by making use of a lead ion selective electrode (ISE). [17]

It came to mind that the only indirect method of analysis of phosphate in a flow injection system was the use of the lead ISE. [17] For the determination of sulphate however, various publications were found where sulphate was determined indirectly on the atomic absorption spectrophotometer (AAS). This was done by adding excess amounts of exactly known amounts of barium(II) ions to the sulphate solution. The barium signal was then used as an indirect indication of the sulphate concentration. The detection of the excess barium was usually done by filtering the precipitate and determine the barium on an AAS. [18 - 20]. Van Staden and Van Rensburg [21] had a different approach. This group used a dialyser equipped with a passive membrane instead of filtering the precipitate. The excess barium ions dialysed across the membrane to the acceptor channel while the precipitate was transported to waste. The barium dialysate was allowed to react with methylthymol blue to form a complex which was measured spectrophotometrically. The latter method had the advantage above the other methods in the sense than no maintenance of the dialyser was necessary whilst the methods using filters, the filters had to cleaned from time to time (that is if the system is not equipped with a modern self cleaning filter).

It was decided to investigate the applicability of both direct and indirect methods of determination. The major prerequisites for the method of choice for use was that it must be simple to use in a flow injection system with the minimum number of interferences. The use of the detection method was secondary to the process that took place in the electrodialyser. For this reason the phosphomolybdenum method for direct determination was chosen. For the indirect method the AAS detector was chosen for use in tandem with an electrodialysing unit.

7.2 Experimental

The experimental section is divided into two parts namely for the indirect determination of phosphate and the direct determination of phosphate.

7.2.1 Indirect determination of phosphate

7.2.1.1 Reagents and solutions

All reagents were prepared from analytical grade chemicals unless otherwise specified. Deionised water from a Modulab system (Continental Water Systems, San Antonio, TX) was used for dilution. All solutions were degassed before measurement with a water vacuum pump system. The main solutions were prepared as follows:

7.2.1.1.1 Standard barium solution

A standard stock barium solution containing 10 000 mg ℓ^{-1} (0.0728 mol ℓ^{-1} in Ba^{2+}) was prepared by dissolving 30.33 g of dried barium chloride in water and diluting to 2 ℓ with de-ionized water. Working standard solutions were prepared by appropriate dilutions to cover the working ranges as discussed in the text.

7.2.1.1.2 Standard phosphate solution

A standard stock phosphate solution containing 10 000 mg ℓ^{-1} (0.1053 mol ℓ^{-1} PO_4^{3-}) was prepared by dissolving 75.42 g of di sodium phosphate duodeca-hydrate ($Na_2HPO_4 \cdot 12\ H_2O$) in water and diluting to 2 ℓ with de-ionized water. Working standard solutions were prepared by appropriate dilutions to cover the working ranges as discussed in the text.

7.2.1.2 Instrumentation

The FIA system (Figure 7.1) used in this work, was composed from the following components: a six-roller Cenco peristaltic pump rotating at 10 rpm, two Valco (Houston, Texas) 10-port electrically actuated injection valves with sample loops

of 70 and 150 µℓ respectively, a reaction manifold system and a laboratory-made electrodialyser. The electrodialyser used (see Figure 7.2) was a slightly modified version of the dialyser unit as described by Van Staden [22, 23]. The dialyser unit consisted of two, mirror image, PVC blocks. Embedded into each of these blocks were graphite electrodes which acted as the cathode (acceptor side) and the anode (donor side) respectively. Placed onto each of the PVC blocks was a 0.6 mm thick Perspex blade. Into each of the Perspex spacer, a groove of 0.6 mm diameter and 300 mm length was cut so as to form a channel when placed onto each of the PVC blocks respectively. The PVC blocks were then fitted onto each other in such a way that the Perspex spacer facing each other and the grooves in the respective Perspex blades coincided with each other. The membrane was then sandwiched between the two Perspex spacer as the only separation between the two tubes so formed. The walls of the tubes that were formed thus consisted of, at the far end, the graphite (which was embedded into the PVC blocks), the side walls of Perspex and the common wall, the membrane. A Leader LPS 156 potentiostat was used to apply the d.c. potential. The passive membrane used was a Technicon pre-mount type C membrane (pore size 4-6 nm, thickness 0.015mm). Tygon tubing (0.76 mm id) was used to construct the manifold system. For current and potential measurements a Prema 5000 integrating multimeter was used. The detector used was a Varian (Palo Alto, CA, USA) AA-1275 atomic absorption spectrometer. A Varian Techtron Ba hollow cathode lamp, operating with a current of 8 mA, was used to give a monochromatic light ray in the detector. A wavelength of 554.0 nm and a spectral bandpass of 0.2 mm was used. A dinitrogen oxide-acetylene flame (reducing) was used. The spectrometer and the injection valve were coupled to a personal computer equipped with the FlowTEK program [24].

7.2.1.3 Flow system

The flow system used is depicted in Figure 7.1. Phosphate sample solutions were drawn up into a 70 µℓ sample loop of the Valco valve (valve 2 Figure 7.1) and barium standard solution was drawn up into a 150 µℓ loop of the Valco valve (valve 1 Figure 7.1) Both the phosphate and the barium were injected at the same time into two separate water streams. The two water streams then converged into one stream (forming the donor channel) where the following precipitation reaction between the phosphate and barium ions took place:

$3\ Ba^{2+}\ (aq) + 2\ PO_4^{3-}\ (aq) \rightleftharpoons Ba_3(PO_4)_2\ (s)$ with a K_{sp} at standard conditions for the reaction being 1×10^{-54}.

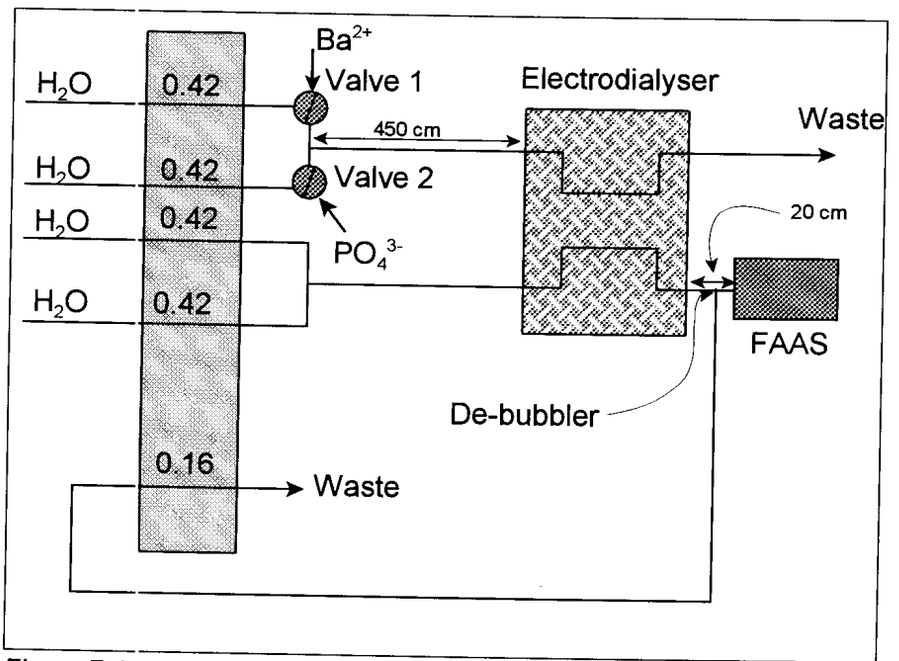

Figure 7.1 Flow system for the indirect determination of phosphate.

Barium ions were in excess. The barium/phosphate precipitate and barium ions which did not react with the phosphate ions were transported to the electrodialyser. In the electrodialyser the barium ions migrated (under the influence of an applied d.c. potential) across the membrane to the acceptor channel whereas the barium/phosphate precipitate was transported to waste. The electrodialysate barium ions were swept from the electrodialyser unit (acceptor channel) and transported to the spectrometer were the barium signal was measured as an indirect indication of the phosphate concentration.

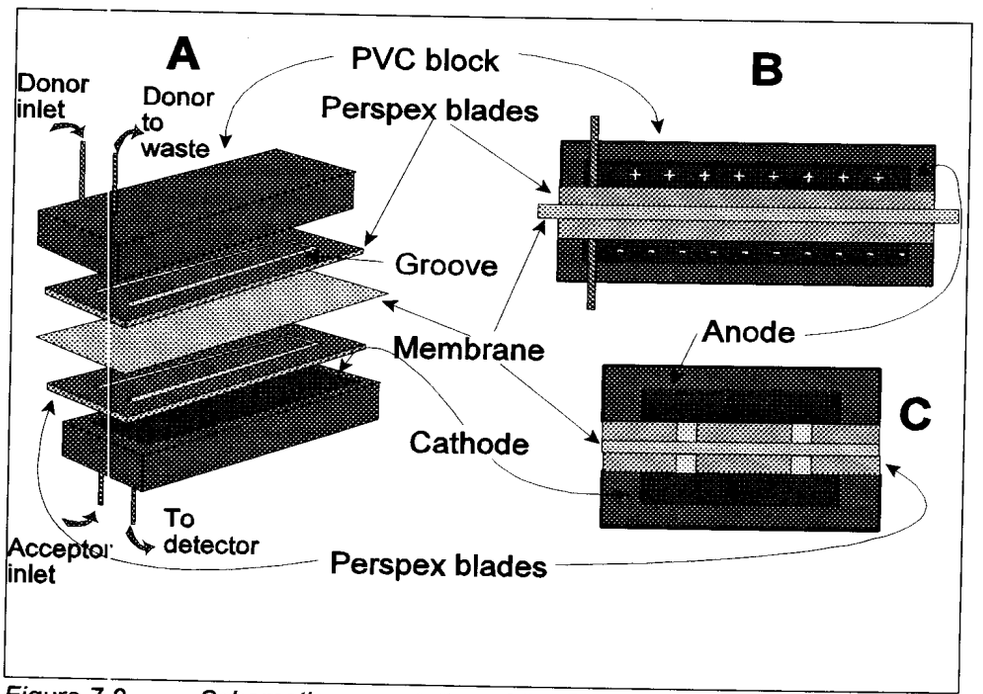

Figure 7.2 *Schematic presentation of the Electrodialyser unit. A - the 3D presentation, B - a longitudinal cross-section and C - a diagonal cross-section.*

Data acquisition and device control were achieved using a PC30-B interface board (Eagle Electric, Cape Town, South Africa) and an assembled distribution board (MINTEK, Randburg, South Africa). The FlowTEK [24] software package (obtainable from MINTEK) for computer aided flow-analysis was used throughout for device control and data acquisition. All the data given (mean peak area values) are the average of 11 replications.

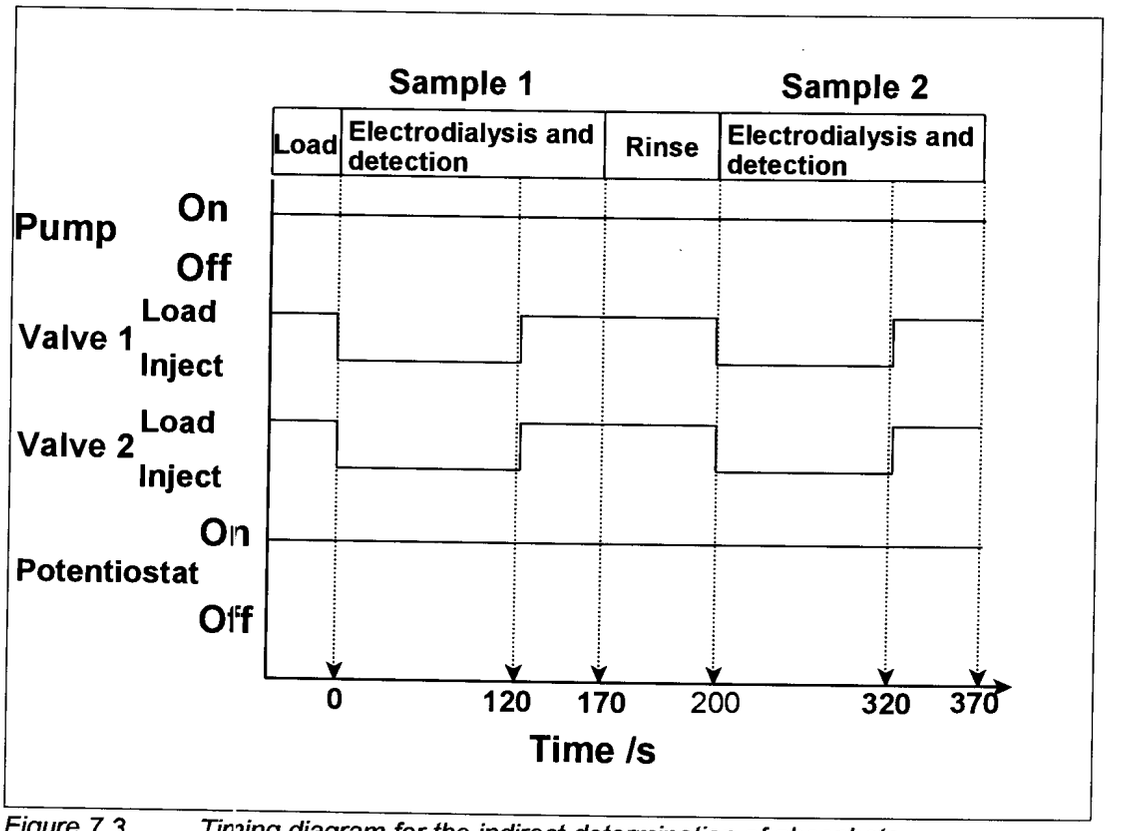

Figure 7.3 Timing diagram for the indirect determination of phosphate.

7.2.1.4 Procedure

The configuration of the FI system is shown in Figure 7.1. The pump and valves operated as described below:

5.2.1.4.1 Operation of pump and valves

The pump (Figure 7.1) was never switched to the "off" position during the analysis. Two Valco 10-port electrically actuated injection valves (valves 1 and 2 in Figure 7.1) were used to inject the barium standard solution and the phosphate sample solution at the same time. In the "load" position (on both valves), sample phosphate solution and barium standard solution were aspirated through the respective sample loops to waste, filling the whole sample loop (phosphate sample solution filled loop in valve 2 and barium standard solution

filled loop in valve 1). Upon switching both valves to the "inject" position, parts of the respective water streams were interrupted and the full sample loops were placed into the respective water streams.

The timing diagram for treating the samples is outlined in Figure 7.3. The system was switched on and allowed to run for about 10 min in order to equilibrate the flow dynamics of all parts of the system. The computer was then actuated and the timing sequence started in the "load" position which was only used at the beginning of the analysis. The following timing sequences were followed with time regulation from the FlowTEK [24] program:

i. *Starting of the system (Loading)*

Pump: Pump was switched to the "on" position. The individual water streams were pumped at a rate of 0.42 mℓ min^{-1} and after they merged, the flow rate of the donor stream through the electrodialyser was 0.84 mℓ min^{-1}. Aspiration of the sample and the standard solution into the injection loop was at a rate of 2.9 mℓ min^{-1}.

Valves: Both valves were in the "load" position.

Potentiostat: The potentiostat was set to "on" position at 20 V.

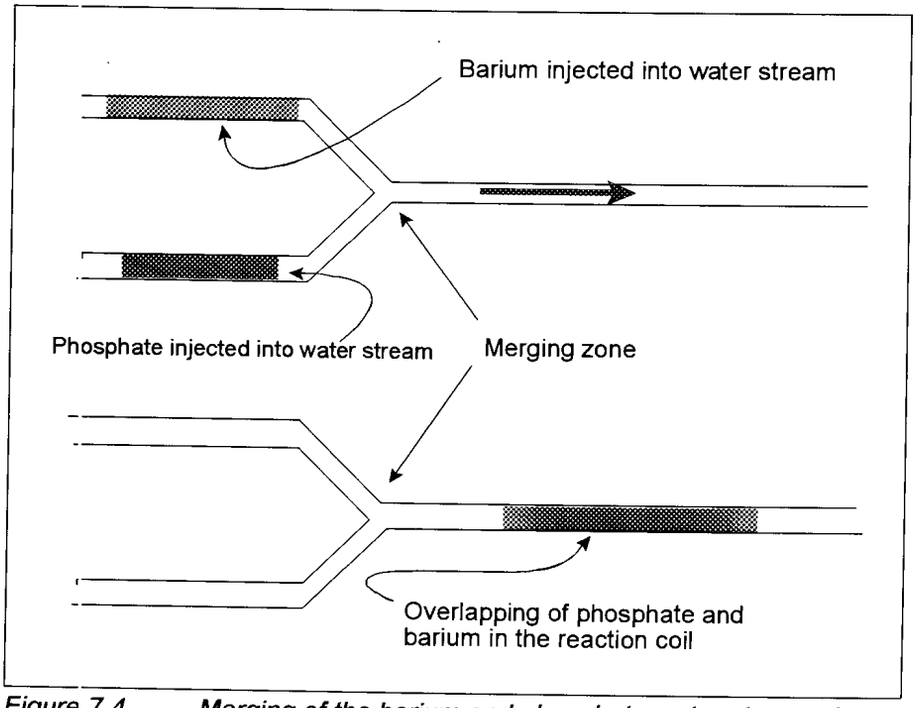

Figure 7.4 *Merging of the barium and phosphate water streams into the reaction coil.*

ii. *Electrodialysis and detection*

At time T = 0, the pump was kept in the "on" position. Both valves were switched to the "inject" position whereupon the whole sample and standard solution loops were placed into the two respective water streams. The sample and the standard plugs were then transported to the donor channel where they merged and the precipitation reaction occurred in the reaction coil. (See Figure 7.4) The precipitate was then transported via the electrodialyser's donor channel to waste whereas the excess barium ions migrated to the acceptor channel. The applied potential over the membrane was kept at 20 V for the duration of the electrodialysing and analysis steps. At time T = 50 s, the computer started reading the signal coming from the detector. The electrodialysed barium ions were pumped to the detector at rate a of 0.84 mℓ min^{-1}. (Flow rate was equal to two times 0.42 mℓ min^{-1} so as to obtain the same flow

rate as in the donor channel since there was not a pump tubing that could deliver 0.84 mℓ min^{-1}). Just prior to the detector a homemade de-bubbler was introduced to remove most of the gases formed at the cathode which interfered with the barium signal. At time T = 120 s, the valves were switched back to the "load" position so as to fill the loops again for the next run.

iii. *Completion of a run*

At time T = 170 s, the computer stopped measuring the signal from the detector. The donor and acceptor channels were rinsed and the next sample was aspirated into the sample loop. At T = 200 s, the two valves were switched to the "inject" position which marked the beginning of analysis of second sample.

7.2.1.5 Results and discussion

In the above mentioned flow system, the reaction of barium with the phosphate, the migration of the barium and the analysis of the barium were the most important considerations for the optimisation. Different from chapters 4, 5 and 6, in this electrodialyser system for indirect determination, it was not the analyte that was electrodialysed but the reactant (barium ions). It was however still very important to ensure the optimum and reproducible transport of the barium across the membrane. The system was thus optimised under the following headings:

i. Concentration of barium.
ii. Applied potential.
iii. Flow rate of the donor and acceptor channels.
iv. Reaction coil.

v. Injection loop volume.

7.2.1.5.1 Barium concentration

For maximum sensitivity of the system it was essential to obtain the optimum working conditions for the determination of the barium ions. For this reason the electrodialysis system was first optimised without the inclusion of any phosphate. The various barium ion concentrations were compared whilst other experimental parameters were kept constant at the following values:

- Concentration phosphate = 0 mg ℓ^{-1} .
- Injection loop volume (Barium) = 100 $\mu\ell$.
- Flow rate (donor and acceptor stream) = 0.84 mℓ min^{-1}.
- Applied d.c. potential = 15 V.

It is clear from Figure 7.5 that there is a steady increase in the peak area with

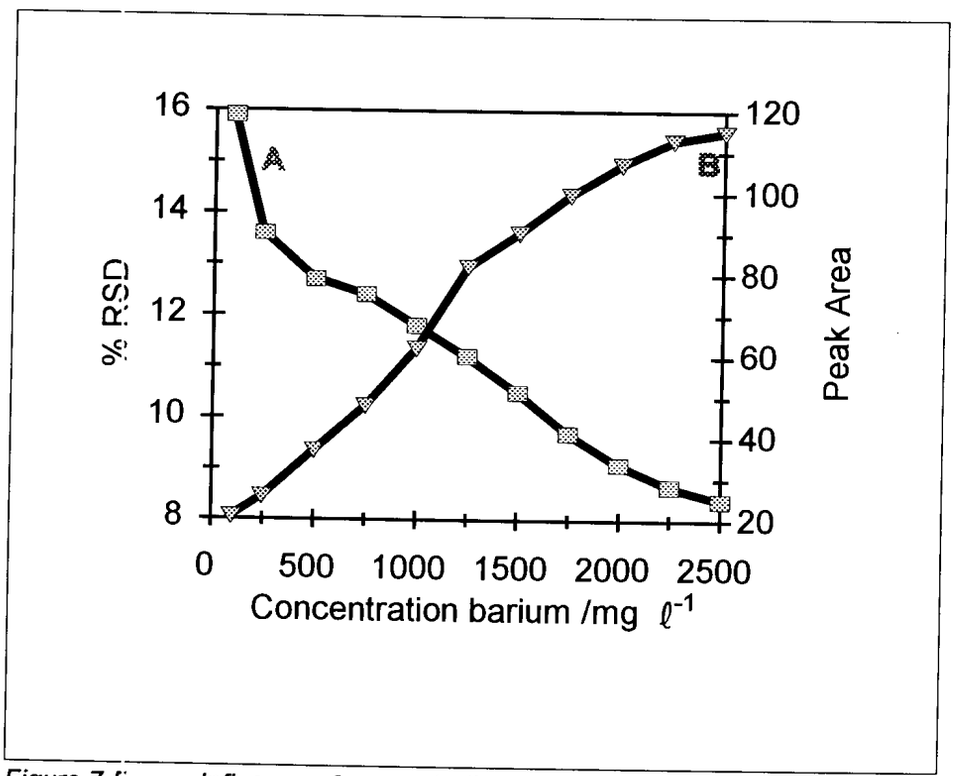

Figure 7.5 Influence of concentration of barium on % RSD (A) and peak area (B).

increasing barium concentration. On the other hand there was a steady decrease in the % RSD with increasing barium concentration. Since reproducibility was a problem in the experimental work a compromise was reached at 2000 mg ℓ^{-1}. At this concentration the reproducibility was relatively low and the sensitivity was acceptable.

7.2.1.5.2 Applied potential

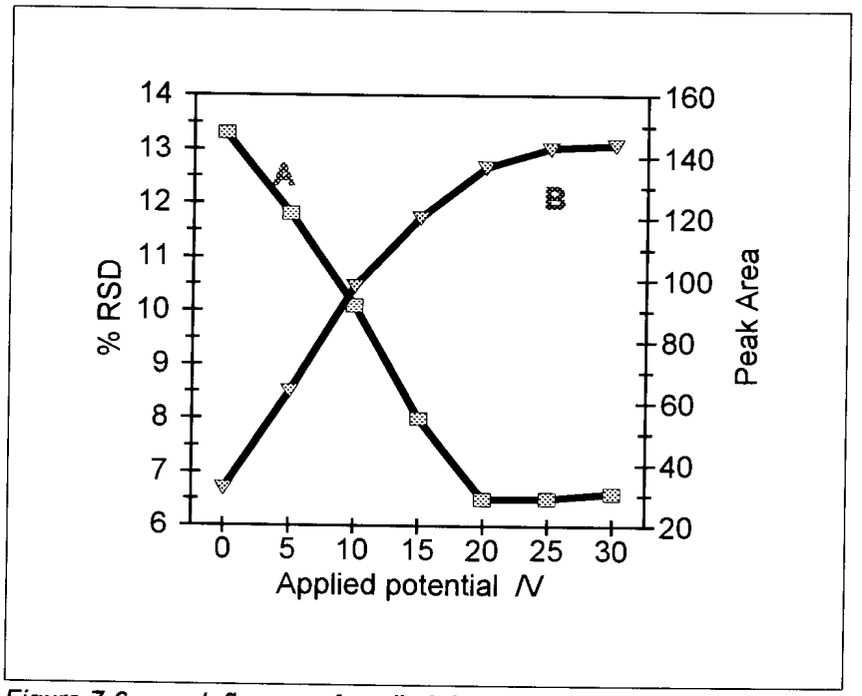

Figure 7.6 *Influence of applied dc potential on the % RSD (A) and the peak area (B).*

The sensitivity and reproducibility of the electrodialysed excess barium ions in the electrodialyser unit depended on the potential gradient applied on the system. The applied potential was therefore evaluated using the detector signal response and % RSD as indicators. The d.c. potential was varied between 0 and 30 V, while the flow rates in the donor and acceptor streams were kept constant at 0.84 mℓ min^{-1}, the injection loop volumes of the barium and the phosphate were respectively 100 and 80 $\mu\ell$ and the reaction coil was 300 cm.

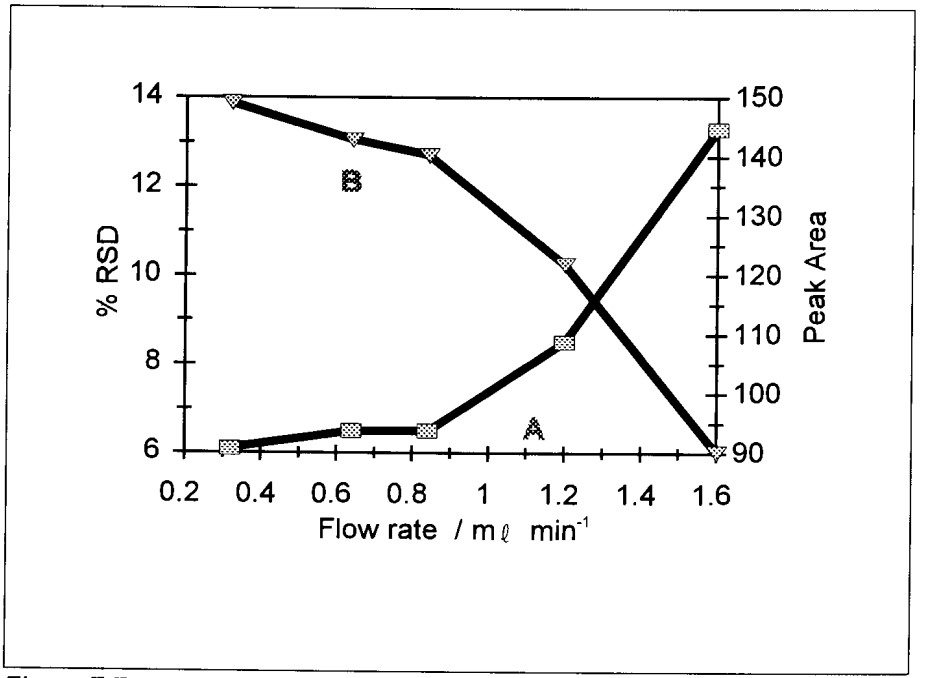

Figure 7.7 *Influence of flow rate on the % RSD (A) and peak area (B). (No phosphate added).*

It should be noted that during this part of the optimisation the concentration of the phosphate was zero so as to obtain the best conditions for the determination of barium. The results in Figure 7.6 revealed that the precision was poor at low applied potentials. This indicated that the contribution of detectable barium ions drawn through the neutral membrane was unstable. It is further clear that there was a steady increase in the peak area with increasing applied potential. This increase however did flatten off after potentials of higher than 20 V were applied. From the graph it is clear that the optimum applied potential was 20 V. With decreasing potential the precision decreased and with increasing potential the precision was constant (respective to 20 V). The sensitivity was also acceptable at 20 V.

7.2.1.5.3 Flow rates of the donor and acceptor streams

Evaluation of the flow rates of both the donor and acceptor streams revealed that the best results were obtained with the flow rates of both streams in the

same direction when applied in the continuous mode. Sensitivity and precision were used as indicators in the optimisation of the flow rates. During these experiments the following experimental parameters were kept constant:

- Phosphate concentration = 0
- Barium ion concentration = 2000 mg $m\ell^{-1}$
- Barium injection loop = 100 $\mu\ell$
- Applied potential = 20 V

The influence of the flow rates was first compared on the basis of %RSD and secondly on the basis of peak area as illustrated in Figure 7.7 It is clear from the results that the precision deteriorated remarkably for flow rates higher than 0.84 $m\ell$ min^{-1}. It is also clear that the sensitivity decreased with increasing flow rate. The reason for the increasing % RSD at higher flow rates is the fact that the barium ions had less time to migrate across the membrane which led to lower signal values and thus a low signal to noise ratio. A possible explanation for the decrease in sensitivity with higher flow rates was that although the flux of ions across the neutral membrane under the influence of the applied electric field remained the same, it could not match the influence of the higher flow rate with dilution effect on the dialysate cations in the acceptor channel of the FIA system. At this point in time it was not possible to make a clear cut decision on what the optimum flow rate will be. To further optimise the flow rate, phosphate was also injected whilst all other experimental parameters were kept constant. The concentration of the phosphate was chosen as it would react in a 2:3 ratio with the barium ions. Thus it was calculated that the concentration of the phosphate (PO_4^{3-}) must be 2075 mg ℓ^{-1}. The results can be seen in Figure 7.8. Considering the peak area, there was a slight increase in the peak area from 0.32 to 0.84 $m\ell$ min^{-1}. At these flow rates the peak areas were considerably lower than the corresponding peak areas in Figure 7.7. This indicated that the precipitation reaction took place and that the available barium ions to migrate across the membrane were considerably less. The increase peak area in

Figure 7.8 from 0.84 to 1.2 mℓ min^{-1} indicated that at the latter flow rate, the precipitation reaction was not complete. Reasons for this could be the fact that there was not enough time for the reaction to go to completion or that at the higher flow rate mixing of the reagents in the reaction coil was incomplete. At flow rates higher than 1.2 mℓ min^{-1}, there was a sharp decrease in the peak area. The reason for this was that even though there were more barium ions available in the donor channel, the ions hadn't had enough time in the donor channel to migrate across the membrane and there was also the higher dilution factor in the acceptor channel due to the increase in the flow rate. The best compromise between sensitivity and precision for employment of the proposed electrodialyser/FIA system was obtained with a flow rate of 0.84 mℓ min^{-1}.

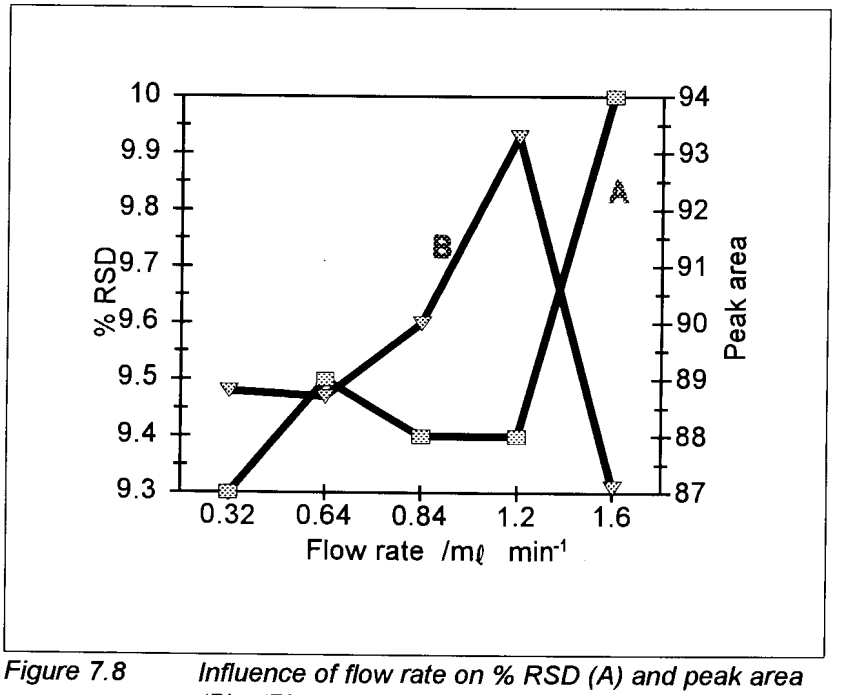

Figure 7.8 *Influence of flow rate on % RSD (A) and peak area (B). (Phosphate added).*

7.2.1.5.4 Reaction coil

As can be seen from the previous paragraph, the reaction time and mixing efficiency was of utmost importance (which was influenced by the flow rate in the previous paragraph). All experimental parameters were kept constant at the following values while the reaction coil length was varied:

- Barium injection loop = 100 $\mu\ell$.
- Phosphate injection loop = 80 $\mu\ell$.
- Barium ion concentration = 2000 mg ℓ^{-1}.
- Phosphate concentration = 2075 mg ℓ^{-1}.
- Flow rate = 0.84 mℓ min^{-1}
- Applied d.c. potential = 20 V

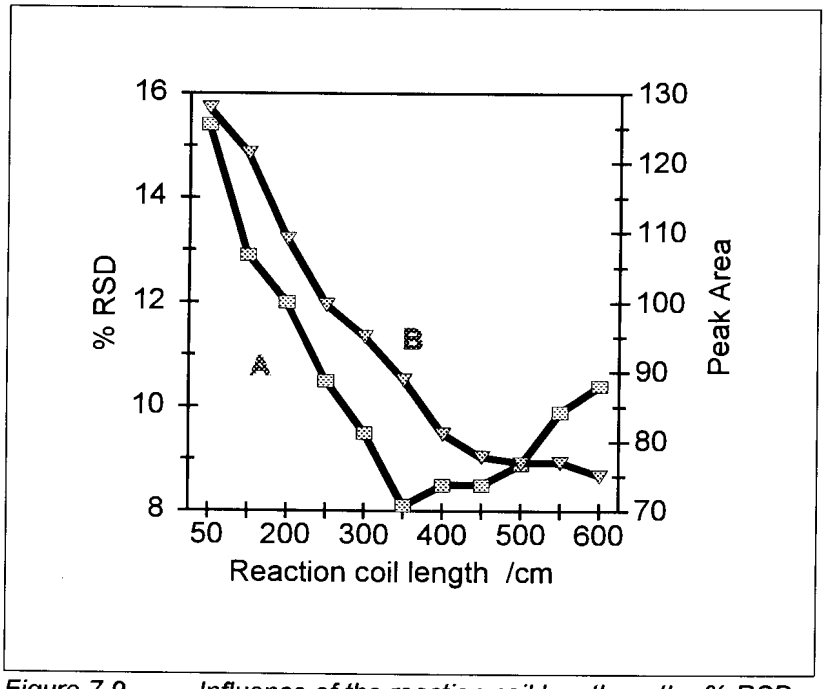

Figure 7.9 *Influence of the reaction coil length on the % RSD (A) and the peak area (B).*

The results can be seen in Figure 7.9. As is evident from Figure 7.9, there was a definite decrease in the barium signal with increasing coil length. This is due

to the better mixing of the reagents and more time for the precipitation reaction to take place with increasing coil length. At lengths longer than 450 cm, there was no significant decrease in the barium signal indicating that the reaction went to completion at a length of 450 cm. The % RSD also showed a steady decrease with increasing coil length up to 350 cm whereafter there was a slight increase in % RSD with increasing coil length. The initial decrease was due to the fact that there was better mixing between the two reagents which led to a more homogeneous mixture and therefore more stable peaks. The increase in the % RSD after 350 cm was due to the fact that there was more time for the excess barium ions to disperse and so very flat and stretched-out peaks were observed. These type of peaks in turn then led to the increase in the % RSD. The optimum length was taken as 450 cm. At 450 cm the barium signal was better than at 350 cm even though the % RSD at 350 cm were slightly better than at 450 cm.

7.2.1.5.5 Injection loop volumes

For the optimisation of the injection loops it was firstly important once again to obtain the optimum barium signal. For this reason the injection loop volume of the barium ions was optimised independently from the phosphate and then afterwards the injection loop volume of the phosphate was optimised at the optimised barium injection loop volume.

For the optimisation of the barium injection loop volume, all the previous experimental parameters were kept constant at their individual optimised values and the concentration of the phosphate was zero. The results can be seen in Figure 7.10. As was expected, there was an increase in the barium signal with increasing injection loop volume. Furthermore it is evident that there is definite decrease in the % RSD at larger injection loop volumes. This is due to the fact

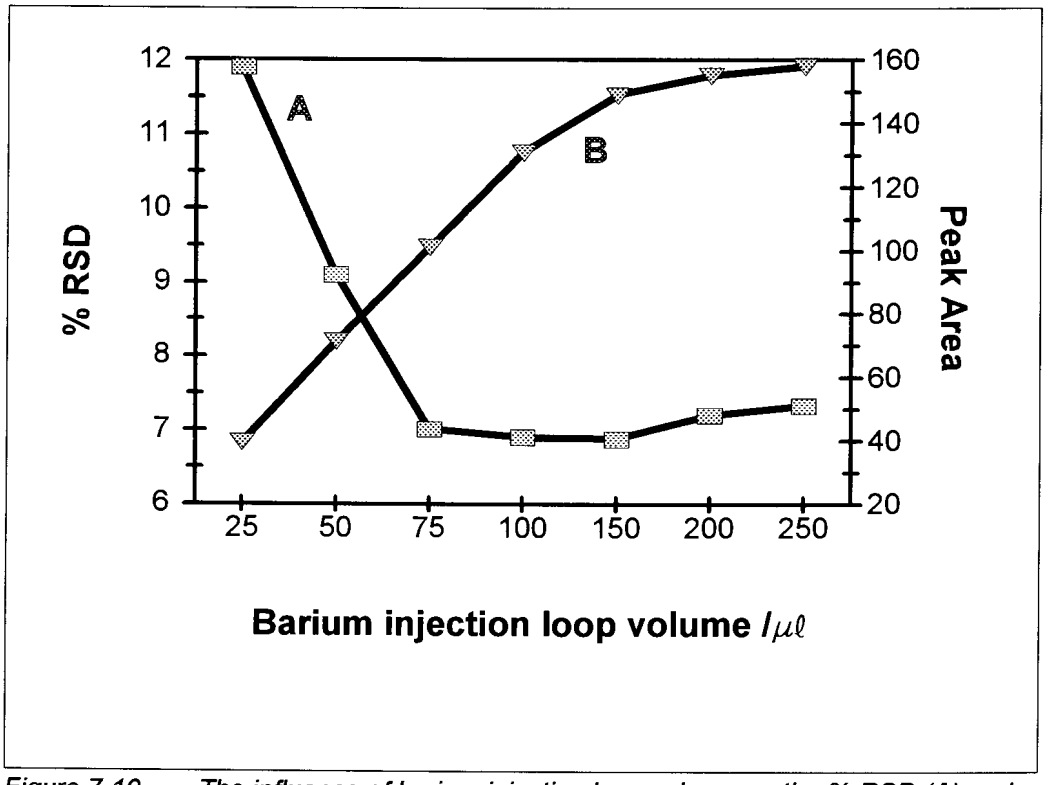

Figure 7.10 *The influence of barium injection loop volume on the % RSD (A) and the peak area (B). Concentration of phosphate was zero.*

that the greater the barium signal, the better the signal to noise ratio will be. The optimum was taken at 150 $\mu\ell$.

During the optimisation of the phosphate injection loop, all experimental parameters were kept constant as with the optimisation of the barium injection loop volume. The barium injection loop volume was kept constant at 150 $\mu\ell$ and the phosphate (PO_4^{3-}) concentration was 2075 mg ℓ^{-1}. From Figure 7.11 it is clear that the barium signal decreased sharply with increasing phosphate injection loop volume up to a volume of 70 $\mu\ell$. Thereafter there was only a gradual decrease in the barium signal. It is further clear from Figure 7.11 that the % RSD increased with increasing injection loop volume. This increase in the % RSD was once again due to the of the barium signal to noise ratio.

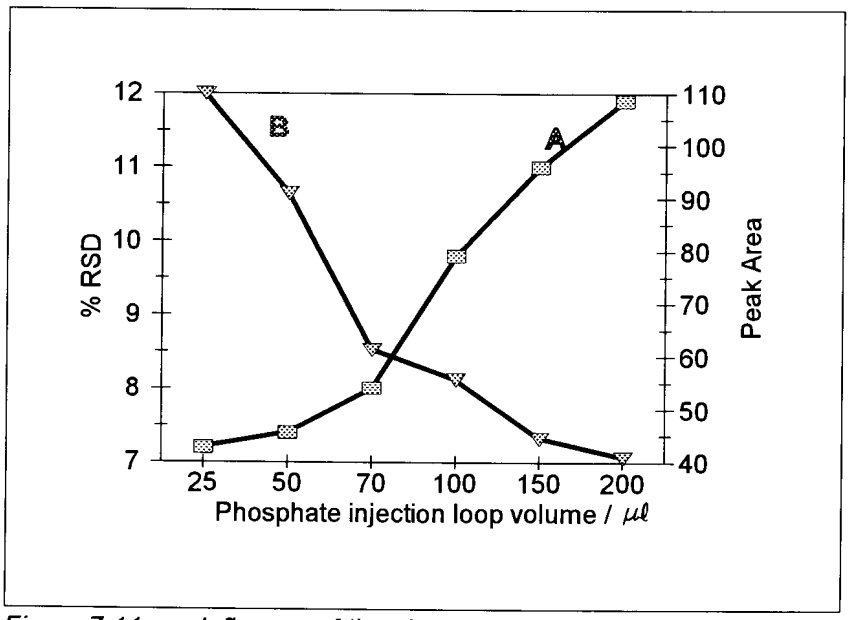

Figure 7.11 *Influence of the phosphate injection loop volume on the % RSD (A) and the peak area (B).*

Other experiments were also done to investigate the influence of the overlapping of the barium and the phosphate zones in the reaction coil. This was done by changing the respective injection loop volumes and changing the concentrations of the barium and the phosphate such that the barium was always in excess. The configurations used are depicted in Figure 7.12. When the overlapping configuration was as indicated in Figure 7.12 C (phosphate zones overlap those of the barium), lower detection values were obtained but the resolution between two different phosphate concentrations were very bad. For this reason the configuration as shown in Figure 7.12 A was preferred.

7.2.1.5 Data and calibration of the optimised system

The optimised parameters for the proposed electrodialysis-FI-AAS analyser for the indirect determination of phosphate were as follows:

- Barium ion concentration: 2000 mg ℓ^{-1}
- Flow rates of donor and acceptor channel: 0.84 mℓ min^{-1}
- Applied d.c. potential: 20 V
- Barium injection loop volume: 150 $\mu\ell$
- Phosphate injection loop volume: 70 $\mu\ell$
- Reaction coil length: 450 cm

The performance of the proposed analyser was critically evaluated under the optimum conditions. The calibration graph was linear between 450 and

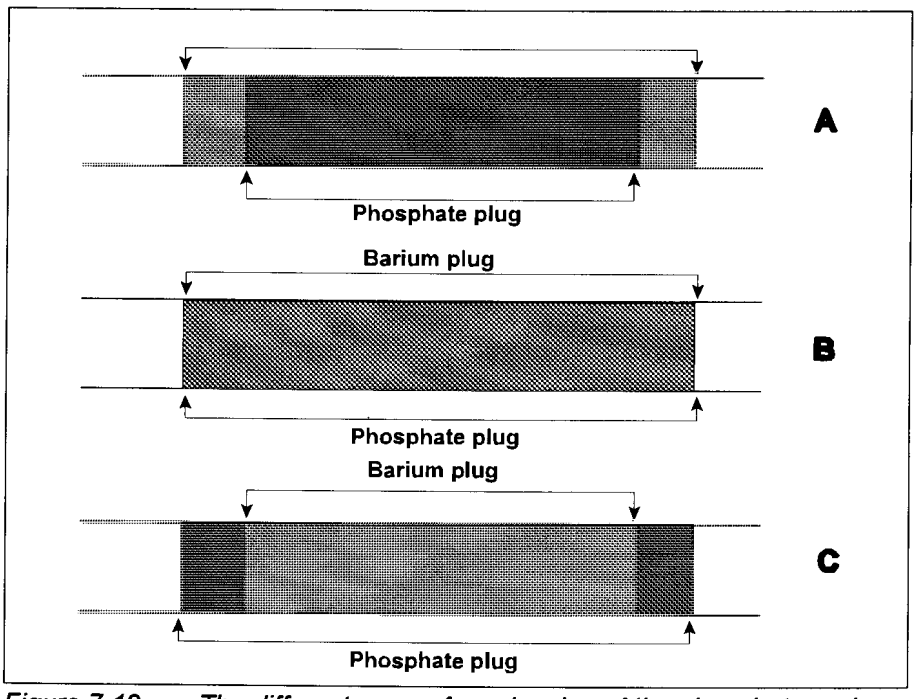

Figure 7.12 The different ways of overlapping of the phosphate and barium zones in the reaction coil.

1750 mg ℓ^{-1} with a relationship between peak area and phosphate concentration given by the following equation:

$$y = -0.9778x + 230.1,$$

where y = peak area and x = phosphate ion concentration in mg ℓ^{-1}. A linear regression coefficient, the variance (r^2) of 0.9778 (n=11) was obtained over this concentration range. The number of runs per hour for the proposed system was 18. The detection limit was calculated to be 413.5 mg ℓ^{-1}, and the sample interaction as 0.98%. The detection limit and the sample interaction was calculated by using the following two equations:

$$\text{Detection limit} = \frac{3(S_b + I_b) - k}{m} \qquad 7.2$$

S_b: is the standard deviation of the background signal

I_b: is the relative peak area of the background signal

k: is the intercept of the calibration curve

m: is the slope of the calibration curve

$$\text{Interaction} = \left(\frac{A_3 - A_1}{A_2}\right) \times 100 \qquad 7.3$$

A_1: is the true peak area of the sample with low analyte concentration, or in other words, the peak area obtained from a stable background.

A_2: is the true peak area of sample containing ten times more analyte than in A_1

A_3: is the peak area for the interacted sample containing the same concentration of analyte as A_1

7.2.2 Direct determination of phosphate

7.2.2.1 Reagents and solutions

All reagents were prepared from analytical grade chemicals unless otherwise specified. Deionised water from a Modulab system (Continental Water Systems, San Antonio, TX) was used for dilution. All solutions were degassed before measurement with a water vacuum pump system. The solutions were prepared as follows:

7.2.2.1.1 Standard phosphate solution

A standard stock phosphate solution containing 10 000 mg ℓ^{-1} (0.1053 mol ℓ^{-1} PO_4^{3-}) was prepared by dissolving 37.71 g of di-sodium phosphate duodeca-hydrate ($Na_2HPO_4 \cdot 12\ H_2O$) in water and diluting to 1 ℓ with de-ionized water. Working standard solutions were prepared by appropriate dilutions to cover the working ranges as discussed in the text.

7.2.2.1.2 Colour reagent

The colour reagent consisted of two solutions namely the reducing agent and the molybdenum solution.

i. Reducing agent solution.

0.1061 g Tin chloride di-hydrate ($SnCl_2 \cdot 2\ H_2O$) and 2.60 g $N_2H_6SO_4$ (hydrazine sulphate) were dissolved in one litre of 0.5 mol ℓ^{-1} sulphuric acid. Sulphuric acid solution was prepared by diluting 27.6 mℓ concentrated sulphuric acid (98 %) to 1 ℓ.

ii. Molybdenum reagent solution.

14.6 g of $(NH_4)_6Mo_7O_{24} \cdot 4\ H_2O$ was dissolved in 1 ℓ of a 0.63 mol ℓ^{-1} sulphuric acid solution (35 mℓ of 98 % sulphuric acid solution diluted to 1 ℓ). To this solution was added 2 mℓ of a sodium laurel sulphate solution. The sodium laurel sulphate solution was prepared by dissolving 17.6 g of sodium laurel sulphate into 100 mℓ water.

7.2.2.1.3 Electrolyte solution

A 4 mol ℓ^{-1} potassium nitrate electrolyte solution was prepared by dissolving 404.44 g of dried potassium nitrate(KNO_3) in water and diluting to 5ℓ with de-ionized water. Working solutions were prepared by appropriate dilutions to cover the working ranges as discussed in the text.

7.2.2.2 Instrumentation

The FIA system (Figure 7.13) used in this work, was composed from the following components: a six-roller Cenco peristaltic pump rotating at 10 rpm, one Valco (Houston, Texas) 10-port electrically actuated injection valve with a sample loop of 80 μℓ, a reaction manifold system (with an i.d. of 0.76 mm) and a laboratory-made electrodialyser. The electrodialyser used was similar to the one used for the indirect determination of phosphate (see Figure 7.2) with the only difference that the cathode was situated in the donor channel and the anode in the acceptor channel. A Leader LPS 156 potentiostat was used to apply the d.c. potential. The passive membrane used was a Technicon pre-mount type C membrane (pore size 4-6 nm, thickness 0.015mm). Tygon tubing (0.76 mm i.d.) was used to construct the manifold system. For current and potential measurements a Prema 5000 integrating multimeter was used. The detector used was a Unicam 8625 UV/VIS spectrophotometer equipped with a 10 mm Hellma-type flow-through cell (volume 80 μℓ). The wavelength of

operation was 660 nm. The spectrometer and the injection valve were coupled to a personal computer equipped with the FlowTEK program [24].

7.2.2.3 Flow system

The flow system used is depicted in Figure 7.13. Sample solutions were drawn up into a 90 μℓ sample loop of the Valco valve from where it was injected into the carrier donor stream and transported into the electrodialyser. Analytes in the sample donor stream were electrodialysed under the influence of an applied d.c. potential through the passive neutral membrane to the acceptor channel. The electrodialysate ions were swept from the electrodialyser unit and mixed with molybdenum chromogenic reagent in the reaction manifold system. The following reactions took place:

Phosphate in an acidic medium and excess molybdate reacts to form molybdophosphoric acid. During a selective reduction of this acid a product with an intense blue colour is formed. The intensity of this colour is proportional to the phosphate concentration. This method is based on the following reactions: [25]

$$H_3PO_4 + 12\ H_2MoO_4 \rightarrow H_3P(MoO_{40}) + 12\ H_2O$$

$$Mo(VI) + \text{reducing agent} \rightarrow Mo(V)\ \text{(slow reaction)}$$

The second reaction is the rate determining step.[1] There was a choice of two reducing agents for use namely ascorbic acid and $SnCl_2$. Even though the ascorbic acid forms a more stable reduction product [26] (leading to a higher reproducibility) and the ascorbic acid itself is more stable than the Sn(II). (Sn(II)

[1] This coloured reaction product was transported to the spectrophotometer for measurement at a wavelength of 660 nm. Experimental work done by the author on a diode array spectrophotometer indicated that the peak maximum shifted to longer wavelengths with time. The shift with time was very slow however and all the analysis were done at the abovementioned wavelength.

is easily oxidised by atmospheric oxygen). The Sn(II) was preferred to the ascorbic acid. The reason for this choice was the fact that the reduction reaction rate for the Sn(II) is much higher than for the ascorbic acid which led to better sensitivity and a higher sampling rate. [27]

Data acquisition and device control were achieved using a PC30-B interface board (Eagle Electric, Cape Town, South Africa) and an assembled distribution board (MINTEK, Randburg, South Africa). The FlowTEK [24] software package (obtainable from MINTEK) for computer aided flow-analysis was used throughout for device control and data acquisition. All the data given (mean height values) are the average of 10 replications.

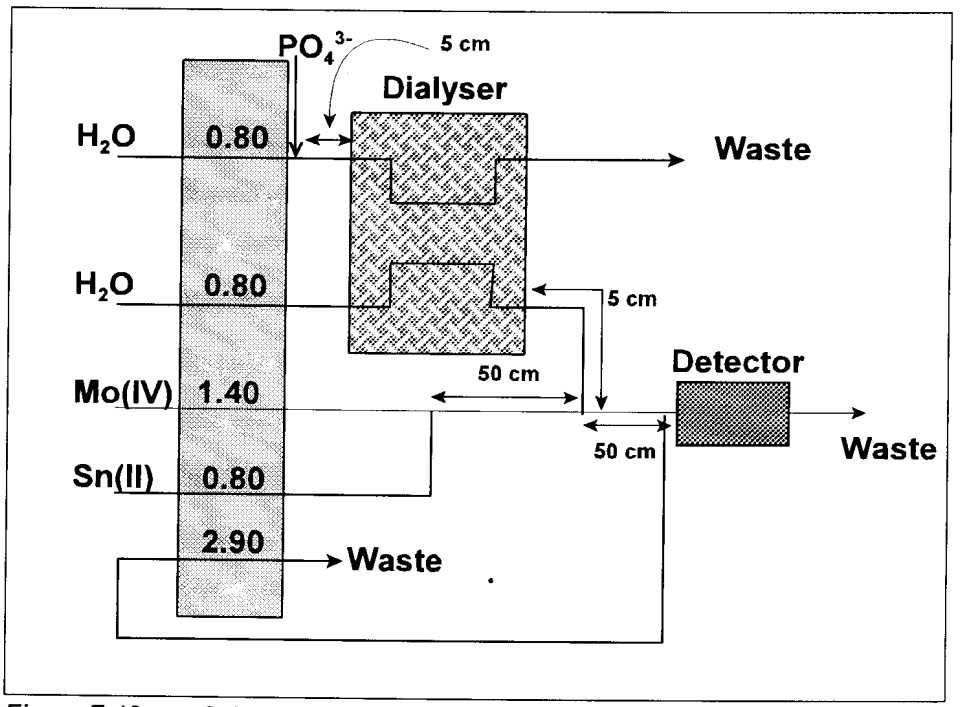

Figure 7.13 *Schematic presentation of the flow/electrodialysis system for the determination of phosphate based on the molybdenum colour reaction.*

7.2.2.4 Procedure

The configuration of the FI system is shown in Figure 7.1. The pump and valves operated as described below.

7.2.2.4.1 Operation of pump and valves

The pump (Figure 7.13) was never switched to the "off" position during the analysis. The Valco 10-port electrically actuated injection valve was used to inject the phosphate sample solution into the water carrier stream. In the "load" position, sample phosphate solution was aspirated through the respective sample loops to waste, filling the whole sample loop. Upon switching the valve to the "inject" position, part of the respective water carrier stream was interrupted and the full sample loop was placed into the water carrier stream.

The timing diagram for treating the samples is outlined in Figure 7.14. The system was switched on and allowed to run for about 10 min in order to equilibrate the flow dynamics of all parts of the system. The computer was then actuated and the timing sequence started in the "load" position which was only used at the beginning of the analysis. The following timing sequences were followed with time regulation from the FlowTEK [24] program:

i. *Starting of the system (Loading)*

Pump: Pump was switched to the "on" position. The carrier donor and acceptor water streams were pumped at a rate of 0.80 mℓ min^{-1}. Aspiration of the sample solution into the injection loop was at a rate of 2.9 mℓ min^{-1}.

Valve: The valve was in the "load" position.

Potentiostat: The potentiostat was set to "on" position at 20 V.

ii. *Electrodialysis and detection*

At time T = 0, the pump was kept in the "on" position. The valve was switched to the "inject" position whereupon the whole sample solution loop was placed into the carrier water stream. The sample plug was then transported to the donor channel of the electrodialyser. In the electrodialyser, under the influence of an applied d.c. potential, the phosphate ions migrated towards the anode in the acceptor channel. The applied potential over the membrane was kept at 20 V for the duration of the electrodialysing and analysis steps. At time T = 45 s, the computer started reading the signal coming from the detector. The electrodialysed phosphate ions were pumped to the detector at rate of 0.80 mℓ min^{-1}. Just prior to the detector a homemade de- bubbler was introduced (operating at a flow rate of 0.16 mℓ min^{-1}) to remove most of the gaseous products formed at the anode which interfered with the phosphate colour product signal. At time T = 100 s, the valve was switched back to the "load" position so as to fill the loop again for the next run.

iii. *Completion of a run*

At time T = 200 s, the computer stopped measuring the signal from the detector. The donor and acceptor channels were rinsed and the next sample was aspirated into the sample loop. At T = 250 s, the valve was switched to the "inject" position which marked the beginning of analysis of second sample.

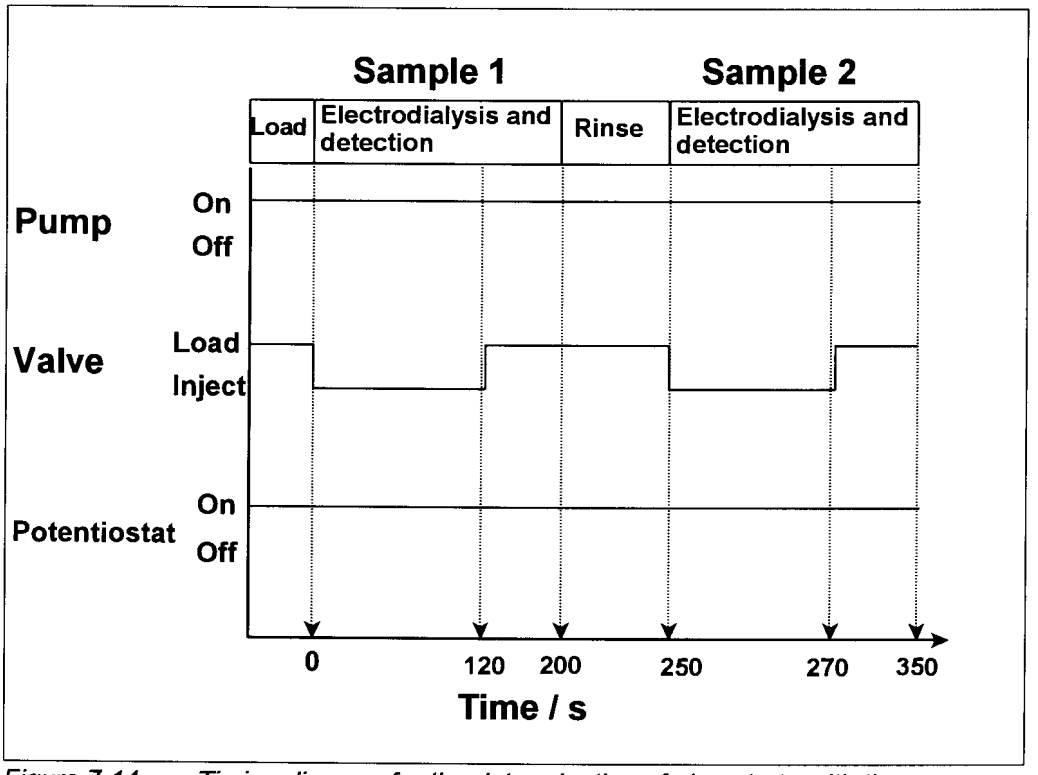

Figure 7.14 *Timing diagram for the determination of phosphate with the molybdenum blue colour reaction.*

7.2.2.5 Results and discussion

Different from the aim of investigation in paragraph 7.2.1, in this section it was the aim to obtain the maximum migration for phosphate through the membrane. The optimisation of this system was for that reason also built round this aim. The determination of the phosphate after dialysis was secondary to the dialysis of the phosphate. For this reason the optimisation and evaluation of the proposed flow system was based upon the factors influencing the phosphate dialysis in the electrodialyser. The following parameters were optimised:

- Flow rate of donor and acceptor channels.
- Applied d.c. potential.
- Injection loop volume.
- Addition of electrolytes to the sample.

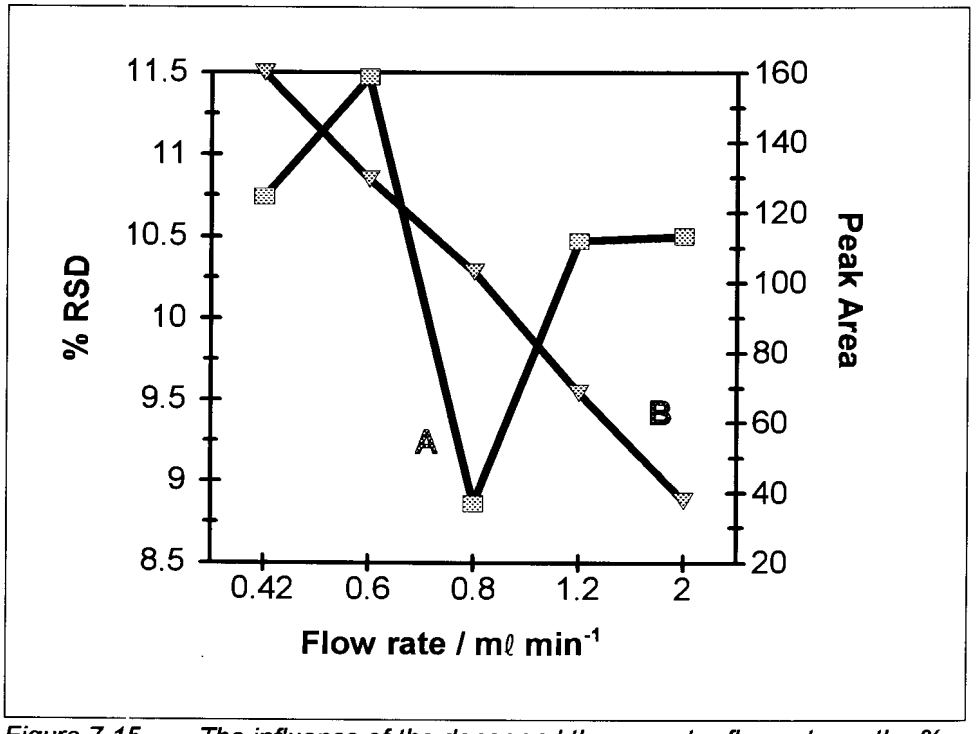

Figure 7.15 *The influence of the donor and the acceptor flow rate on the % RSD (A) and the peak area (B).*

All experimental parameters were evaluated on the basis of % RSD (reproducibility) and peak area (sensitivity).

7.2.2.5.1 Flow rate of the donor and acceptor channels

During the optimisation of the flow rate in the donor and acceptor channels the other experimental parameters were kept constant at the following values:

- Applied d.c. potential: 15 V
- Injection loop volume: 90 $\mu\ell$

The concentration of the phosphate ions was kept constant at 50.0 mg ℓ^{-1}. The donor and the acceptor channels were always flowing at the same rate and it was varied between 0.42 and 2.00 mℓ min^{-1}. The results can be seen in Figure 7.15.

As was expected there was a decrease in peak area with increasing flow rate. The reasons for this is that due to the higher flow rate, less time is available for the phosphate ions to migrate across the membrane. Furthermore, even if the number of phosphate ions that did migrate, the higher flow rate in the acceptor channel led to a higher dilution factor of the dialysate ions. The % RSD also did increase with an increase in the flow rate due to the lowering of the signal to noise ratio. Even though the peak areas at low flow rates compared very favourably with those at the higher flow rates but high % RSD values were obtained at these low flow rates. The high % RSD was due to unstable flow patterns at too low flow rates. (Different from the copper system discussed in Chapter 5, unstable flow will influence zinc system since the zinc will not be plated under these low flow rates. Thus, in the zinc system detection took place during the low flow rates whereas in the copper system plating took place under low flow rate conditions) A flow rate of 0.80 mℓ min^{-1} was a good compromise between too high % RSD values and too low peak areas.

7.2.2.5.2 Applied potential

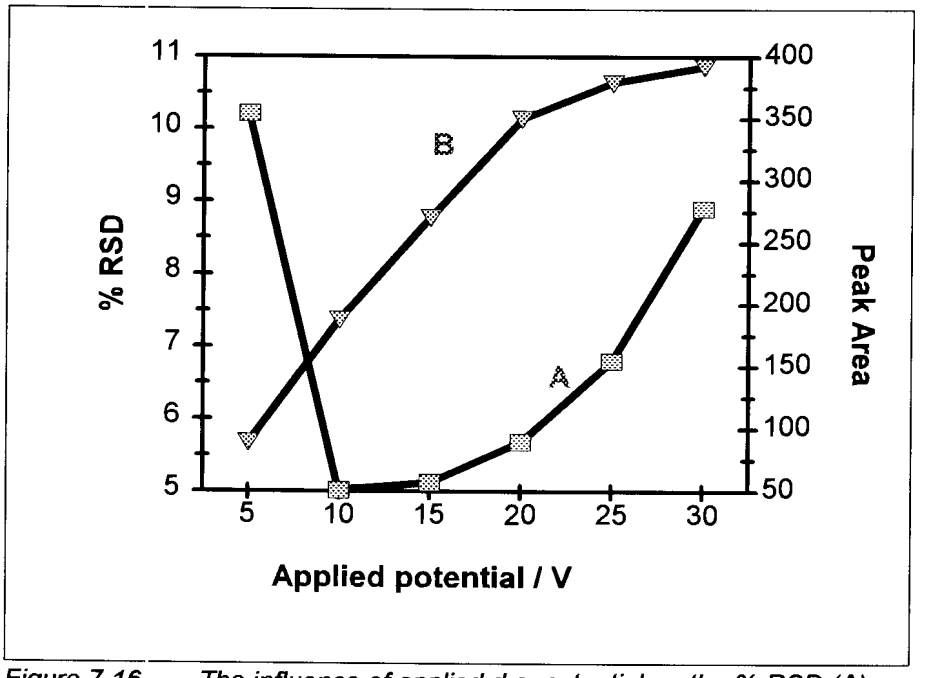

Figure 7.16 *The influence of applied d.c. potential on the % RSD (A) and the peak area(B) for the proposed molybdenum blue colour reaction.*

The applied d.c. potential was proven to be the single most important parameter for an increase in the signal peak area. During the optimisation of the applied d.c. potential all other experimental parameters were kept constant at the following values:

- Flow rate of donor and acceptor channel: 0.80 mℓ min^{-1}.
- Injection loop volume: 80 $\mu\ell$.

The concentration of the phosphate sample was 50 mg ℓ^{-1}. The applied potential was varied between 0 and 30 V. The results can be seen in Figure 7.16. A sharp increase in the peak area was observed with increasing applied potential from 0 to 20 V. After 20 V the increase somewhat flattened off. The reason for this flattening in the peak after 20 V is that it can be assumed that at 20 V most of the phosphate ions will migrate to the acceptor channel. Even though not as obvious as in Figure 7.16, the same can be derived from Figure 7.17. With increasing potential, the number of phosphate ions that migrate will not increase accordingly. The high % RSD value at 5 V is due to the low signal to noise ratio. The increase in the % RSD from 20 V and higher is due to the formation of more gaseous products at the anode than the de- bubbler can

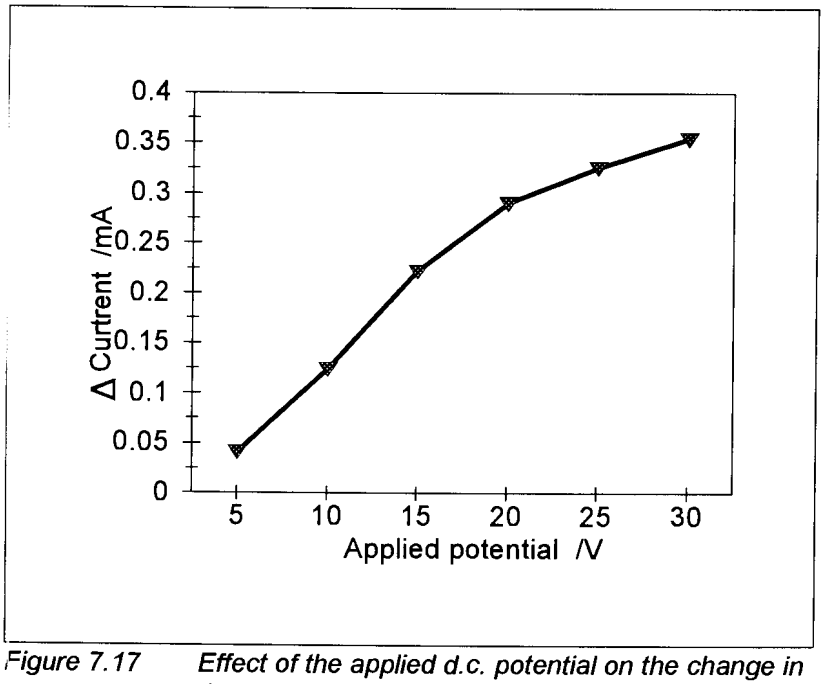

Figure 7.17 *Effect of the applied d.c. potential on the change in the acceptor channel indicating the flux of ions through the passive neutral membrane*

handle. The optimum applied d.c. potential was taken at 20 V.

7.2.2.5.3 Injection loop volume

For the optimisation of the injection loop volume the other experimental parameters were kept constant at the following values:

- Flow rate of donor and acceptor channel: 0.80 mℓ min^{-1}.
- Applied d.c. potential: 20 V.

The concentration of the phosphate sample was 20.0 mg ℓ^{-1}. The results are depicted in Figure 7.18. The optimum volume was taken at 80 $\mu\ell$. Even though the sensitivity was not as high as with the larger volumes, the precision was much better

7.2.2.5.4 Influence of added electrolyte

During the optimisation of the proposed flow/electrodialysis system, perfect

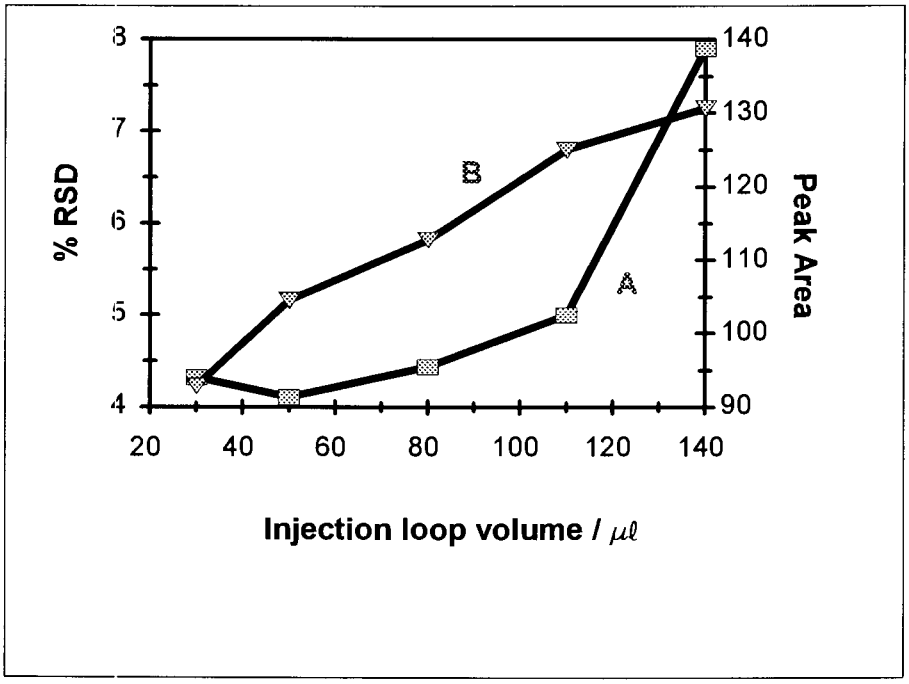

Figure 7.18 Influence of injection loop volume on % RSD (A) and peak area (B).

conditions availed during the optimisation of each experimental parameter. Under normal circumstances when analysing real samples, other electrolytes may also be present in the sample solution. It was therefore of utmost importance to evaluate the influence of electrolyte concentrations on the proposed system. Potassium nitrate was added, in different concentrations, to the sample solution (sample solution phosphate concentration were kept constant at 30 mg ℓ^{-1}). All the experimental parameters was kept at the optimised values. The results are depicted in Figure 7.19. It is clear that electrolyte does have a large influence on the migration of the phosphate ions. As can be seen in Figure 7.19, the peak area increased with increasing electrolyte concentration up to a concentration of 1 mol ℓ^{-1}. After 1 mol ℓ^{-1}, there was no further increase in the peak area with increasing electrolyte concentration. This increase in peak area with increasing electrolyte concentration was due to the fact the phosphate ion was less hydrated and thus the effective radius decreased leading to a smaller viscous drag (implying a higher migration rate across the membrane, see chapter 3). For real samples, electrolyte was added to the samples so that the final electrolyte concentration in the sample was at least 1 mol ℓ^{-1}.

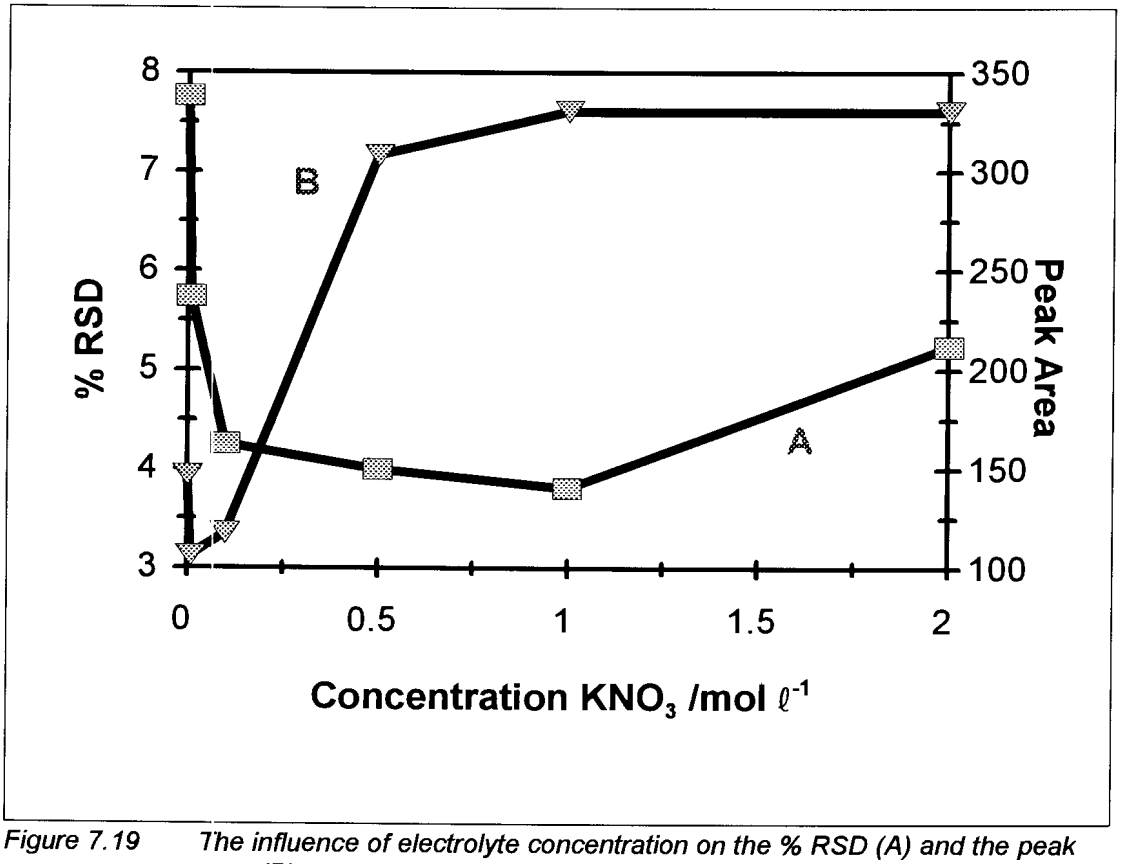

Figure 7.19 *The influence of electrolyte concentration on the % RSD (A) and the peak area (B).*

7.2.2.5.5 Interferences

The most common interferences in the determination of phosphate is Si(IV), Fe(III), Cu(II) and arsenate (AsO_4^{3-}) . [11, 25] What is of interest, was that by making use of the electrodialyser, all cationic interferences were removed. This only left us with the arsenate which was not present in the samples that were analysed.

7.2.2.5.6 Data and calibration of the optimised system

The optimised parameters for the proposed electrodialysis-FI-AAS analyser for the direct determination of phosphate with the molybdenum blue colour reaction were as follows:

- Flow rates of donor and acceptor channel: 0.80 mℓ min^{-1}
- Applied d.c. potential: 20 V
- Injection loop volume: 80 $\mu\ell$
- Minimum electrolyte concentration: 1 mol ℓ^{-1}

The performance of the proposed analyser was critically evaluated under the optimum conditions. The calibration graph was linear between 15 and 200 mg ℓ^{-1} with a relationship between peak area and phosphate concentration given by the equation;

$$y = 1.021x + 102.4, \qquad 7.4$$

where y = peak area and x = phosphate ion concentration in mg ℓ^{-1}.

A linear regression coefficient, the variance (r^2) of 0.997 (n = 11) was obtained over this concentration range. The number of runs per hour for the proposed system was 14. The detection limit was calculated to be 10.27 mg ℓ^{-1}, and the sample interaction as 0.0887%. The detection limit and the sample interaction was determined by making use of equations 7.2 and 7.3 respectively.

7.2.2.5.7 Samples

All samples were prepared in a 1 mol ℓ^{-1} KNO_3 solution. The following samples were analysed:

Sample 1	Shake 'n Grow Fern Food
Sample 2	Grokon Potplant Food
Sample 3	Wonder 3:2:1 (22)
Sample 4	Wonder African Violet Food

The results are depicted in Table 7.1. The fertilisers were dissolved in the electrolyte solution. The amount of fertiliser dissolved depended on the

distributer's note. The phosphate concentration after preparation was ca 70 mg ℓ^{-1}. The distributer's note only indicated the concentration of phosphorus. It can be seen from table 7.1, that all the concentrations obtained with the proposed method corresponded very well with the concentrations obtained with the standard method. For sample 2, it was found that the concentration of phosphate was far to low. The reason for this might be that the phosphorus was not in the ortho-phosphate form.

Table 7.1 *comparison of samples analysed by the proposed system and a standard method of analysis for phosphate.*

Sample	Phosphate concentration / mg ℓ^{-1} (Proposed method)	% RSD	Phosphate concentration / mg ℓ^{-1} (Standard method)
1_a	65.7	5.2	69.9
1_b	67.8	4.9	70.2
2_a	17.3	5.6	17.2
2_b	15.6	5.1	16.9
3_a	72.2	4.5	69.9
3_b	70.9	4.5	70.1
4_a	70.1	4.6	70.7
4_b	69.5	4.7	70.1

7.3 Conclusions

The direct method completely overshadowed the indirect method of phosphate analysis. It is very obvious that the direct determination of phosphate is much more liable for general use than the indirect method of analysis. Very high detection limit for the indirect method made it very difficult to defend this analysis method. High % RSD values for such high concentrations were unacceptable. Thus the sensitivity, precision and the sample throughput of the direct method was much more acceptable. The ease

of use and compatibility of the direct method was also much better than the indirect method.

Concerning the direct method, it was proven to be a very effective way for the determination of phosphate in water solutions. It exhibited a very wide linear response for the peak area versus concentration of phosphate. For this reason a wide range of phosphate concentrations could be analysed without prior dilution or pre-concentration of the sample.

In this Chapter it was also shown that the phosphate ion's drift speed can be changed by adding an electrolyte. By the addition of the electrolyte, the drift speed of the phosphate ion under the influence of the applied d.c. potential increased tremendously due to the fact that the viscous drag caused by the water molecules which encapsulated the phosphate ion. The addition of the electrolyte led to the partial decapsulation of the phosphate ion which led to lower viscous drag and higher drift speeds and thus also a better percentage dialysis.

By comparing the anions analysed with the electrodialyser, it can be seen that the phosphate system was far more superior to the chloride system (Chapter 4). The main reason for this lay in the development of the homemade de-bubbler. As is evident from the results from Chapter 4, the main problem that hampered the detection of the chloride was the gaseous products that were produced at the anode. For this reason it was not possible to work at optimum flow rates for the chloride as was the case with the phosphate.

7.4 References

a: Standard Methods (**1985**) Standard methods for the examination of water and wastewater. 16th ed. American Health Association, Washington.

b: Boolootain R.B., Stiles K.A., (**1981**) College Zoology, Macmillan Publishing Co., Inc., New York

c: Jeannette E., Watson R.N., (**1979**) Medical-Surgical Nursing and related physiology, W.B Saunders Company.

d: Bohinski R.C., (**1987**) Modern Concepts in Biochemistry, 5th ed., Allyn and Bacon Inc.

e: MacLaurin P., Worsfold P.J., Norman P. Crane M., (**1993**) Anal. Proc. 30(3): 134.

f: Shan Y., McKelvie I.D., Hart B.T., (**1993**) Anal. Chem. 65(21): 3053.

g: Spvakov B.Ya., Maryutina T.A., Shipigun L.K., Shkinev V.M., Zolotov Y. A., Ruseva E., Havezov I., (**1990**) Talanta. 37(10): 889.

h: Daykin R.N.C., Haswell S.J. (**1995**) Anal. Chim. Acta. 313(3): 155.

i: Carrer I., Cusmai P., Zanzottera E., Martinotti W., Realini F., (**1995**) Anal. Chim. Acta. 308(1-3): 20.

j: Benson R.L., McKelvie I.D., Hart B.T., (**1994**) Anal. Chim. Acta. 291(3) 233.

k: Benson R.L., McKelvie I.D., Hart B.T., Truong Y.B., Hamilton I.C., (**1996**) Anal. Chim. Acta. 326(1-3): 29.

l: Peat D.M.W., McKelvie I.D., Mathews G.P., Haygarth P.M., Worsfold P.J., (**1997**) Talanta. 45(1): 47.

m: Oshima M., Goto N., Susanto J.P., Motomiza S., (**1996**) Analyst. 121(8): 1085.

n: Motomiza s., Oshima M., (**1987**) Analyst. 112(3): 295.

o: Baba Y., Yosa N., Ohashi S., (**1985**) J. Chromatogr. 318(2): 319.

p: Harden S.M., Nonidez W.K., (**1984**) Anal. Chem. 56(12): 2218.

q: Coetzee J.F., Gardner C.W., (**1986**) Anal. Chem. 58(3): 608.

r: Stock D.J., (**1987**) At. Spectrosc. 8(1): 1.

s: Kokkonen P., Palko M., Lajunen L.H.J., (**1987**) At. Spectrosc. 8(3): 98.

t: Yakuta K., Sagra F., Yoshida I., Ueno K., (**1990**) Anal. Sci. 6(5): 711.

u: Van Staden J.F., Van Rensburg A., (**1990**) S. Afr. J. Chem. 43(3-4): 78.

v: Van Staden J.F., (**1991**) Talanta. 38(9): 1033.

w: Van Staden J.F., (**1995**) Frezenius'. Z. Anal. Chem. 352: 271.

x: Marshall G.D., Van Staden J.F., (**1992**) Anal. Instr. 20 79.

y: Pauer J.J., (**1989**) Die vloei-inspuitanalise van sekere determinante in oppervlak- en grondwater. MSc. dessertation. University of Pretoria.

z: Murphy J., Riley J.P., (**1962**) Anal. Chim. Acta. 27: 1431.

aa: Janse J.A.H.M., Van der Wiel P.F.A., Kateman G., (**1983**) Anal. Chim. Acta. 155: 89.

Chapter 8

Conclusions

As was indicated in Chapter 1, there is an ever increasing demand for better accuracy, lower detection limits, higher sample throughput and the need for automation. Flow injection analysis (FIA) lend itself perfectly to the fulfilment of these demands due to its versatility. FIA were used extensively with a variety of different detectors to fulfil some of the abovementioned requirements. To further improve the performance of FIA it was used in tandem with numerous sample modifying methods. Modifying in the sense of preconcentration, dilution, derivitisations, conversions and sample cleanup so that the detector is able to respond accurately in an acceptable response time. One of these in tandem methods was the use of a dialyser equipped with a passive neutral membrane. This FIA/dialysis tandem system was applied very successfully in automated sample dilution and cleanup systems. Dialysis, however, was found to be a very slow process which gave rise to unacceptably high detection limits. This then led to a tremendous decrease in the applications of passive dialysis systems in tandem with FIA. Since passive dialysis were so easily incorporated into FIA systems, means of circumventing the massive dilution factor, accompanied with passive dialysis, had to be found without reducing the extent of its advantages.

The proposed system kept the dialyser intact and only introduced electrodes in the donor and acceptor channel respectively. By applying a d.c. electrical potential across the membrane then increased the movement of ions from the donor to the acceptor channel. The reasons for the increase in the percentage dialysis from the passive dialyser to the electrodialyser were two fold.

The first reason was the increased concentration on the donor side of the passive membrane (in the case of the electrodialyser. This was due to the migration of ions under the influence of the applied d.c. electrical potential from the bulk of the donor

channel to the surface of the membrane (donor side). The ions accumulated as a thin, highly concentrated analyte layer which of course gave rise to a higher concentration gradient for diffusion across the membrane. In the case of the passive dialyser, the concentration gradient across the membrane was only due to the concentration of the analyte in the sample bolus. Thus the electrodialyser acted as a preconcentration method of the analyte in the acceptor stream which led to a higher concentration gradient across the membrane.

The second reason was the increased movement of ions across the membrane. The movement of ions across the membrane took place due to not only one force, but to two separate forces. The first force for the transport across the passive membrane was the concentration gradient whereas the second force was the electrical potential applied across the membrane.

It was found that the percentage dialysis increased from ca 7% in passive dialysis to over 90% in some applications (the proposed electrodialysis system). The dilution factor was reduced to a large extent. In the electrodialysis system it was possible to introduce controllable dilution without changing the surface area of the membrane. This was accomplished by changing the applied d.c. electrical potential to suit the specific need.

The advantage in the passive dialysis system of sample cleanup was retained in the proposed electrodialysis system. It was found that the electrodialyser was capable of discriminating against opposite charge (opposite in charge to the analyte) and neutral interferences. Interferences of opposite charge to the analyte migrated away from the membrane and were then kept in the donor channel. The interference from neutral species were diminished to a very large extent. Since the neutral species did not migrate under the influence of the applied d.c. electrical potential, the transfer of these species to the acceptor channel were minimal. Even though some neutral species could have diffuse to the acceptor channel due to the concentration gradient, the

transfer of analyte ions was far more superior to the transfer of neutral interfering species.

Comparison of the passive dialysis system to that of the electrodialysis system can be taken a step further. In passive dialysis, preconcentration of the analyte can be done only outside the dialyser unit. On the other hand, in the case of the electrodialyser, it was possible to preconcentrate the analyte in the dialyser unit itself. (The electrodialyser unit could thus be used as an analyte preconcentration tool). The reduction of a metal analyte ion made it possible to preconcentrate the analyte on the cathode in the acceptor channel. This led to a tremendous decrease in the detection limit of the system in which it was possible to reduce the metal analyte cation.

Unfortunately we are not living in the perfect world. Many problems arose with the development of the electrodialyser system, many of which we were able to reduce to certain extents.

The introduction of the electrodialyser unit into the FIA system was very troublesome. Tremendous problems were experienced with the initial development of the electrodialyser unit and the initial introduction thereof into the FIA system. Choices were to be made of types of electrode- and electrodialyser unit materials. Experiments were done on the physical dimensions of the electrodialyser unit. Changing and fitting of the membranes and the cleaning of the electrodialyser unit took very long periods of time. Due to reactions that took place at the electrodes during analysis, erosion of the electrodes took place. Small particles of the electrodes led to blockages of the FIA system and sometimes also interfered in the detector. The blockage problem forced the use of larger than necessary couplings to the electrodialyser unit which led to increased dispersion.

One of the first problems encountered was in the use of electrochemical detectors with the electrodialyser unit. The use of electrochemical detectors showed very poor

results. No matter how well the electrodialyser unit was grounded, interferences occurred in these type of detectors. Low precision and large baseline drift was experienced. This reduced the versatility of the FIA/electrodialysis system to a large extent.

Another problem encountered was the formation of gaseous products at the electrode in the acceptor channel. These gaseous products caused major problems in the UV/Vis spectrophotometric detectors and to a lesser extent in the Flame atomic absorption spectrometer. This necessitated for higher than optimum flow rates in the dialyser unit which led to higher dilution of the dialysate in the acceptor channel, lower mass transfer rates and in the long run higher detection limits and a poor precision. Even though the homemade de-bubbler used, removed much of the gaseous products, it did not solve the problem completely. The de-bubbler had a slow-moving stream area (to allow the gas bubbles to separate from the liquid) which increased the dead volume and of course led to an increased dispersion.

In conclusion one can make the following comments: The newly developed electrodialysis system can be introduced into a laboratory for routine analysis. Full advantage must be taken of its superior application (superior to passive dialysis) in FIA systems. Care must however be taken to minimise factors leading to dispersion of analyte samples. Time must also be allowed for the development of each individual application.